P145134.PDF [Page: 4 of 53]

Contractors Report 94-64

Analysis of Acoustic Data from The Heard Island Feasibility Test Pertaining to the Canadian Receiving Stations

Prepared by

Paul Scrimger, Ian Schumacher
JASCO Research Ltd., Sidney B.C.

JASCO Research Ltd.
9865 W. Saanich Road
Sidney, B.C. V8L 3S1
(604) 656-0656

Scientific Authority
Dr. Garry Heard
Defence Research Establishment Pacific
FMO Victoria, B.C.,V0S 1B0

Contract Serial No. W7708-2-0518/01-XSA

©DEFENCE RESEARCH ESTABLISHMENT PACIFIC
Research and Development Branch
Department of National Defence

June 1994

Acknowledgements

The following report is one of a series of Contractor Reports on the analysis of the data from the Heard Island Feasibility Test which was performed under Contract No. W7708-2-0518/01-XSA - ***An Acoustic Ocean Thermometer for Detection of Global Warming,*** awarded in response to an Unsolicited Proposal to the Environmental Innovation Program of Supply & Services Canada and supported by the sponsors listed below:

Environmental Innovation Program
Department of National Defence (Defence Research Establishment Pacific)
Department of National Defence (Defence Research Establishment Atlantic)
Department of Fisheries & Oceans (Institute of Ocean Sciences)
Environment Canada (Atmospheric Environment Service)
Province of BC (Ministry of Advanced Education, Training & Technology)
Province of BC (Department of the Environment)
JASCO Research Ltd., who made a financial contribution by foregoing their profit

JASCO Research Ltd. would like to acknowledge the deep interest and generous financial contributions made by all of the sponsors to this very valuable environmental research project.

We would also like to acknowledge the valuable assistance provided to JASCO's research team by Drs. Ross Chapman and Garry Heard of DREP and Dr. Ian Fraser of DREA.

1. Introduction

This report provides a summary of the acoustic data associated with the Canadian measurements taken during the Heard Island Feasibility Test. It is the sixth and final report in a series of reports and journal articles which have been produced under DSS contract no. W7708-2-0518/01-XSA. The other reports produced under this contract included a summary of non-acoustic data from the Heard Island Feasibility Test pertaining to the Canadian receiving stations [1], three consecutive articles submitted to JASA [2-4] describing novel signal processing techniques developed during the course of this work and a DREP contractors report [5] which investigated the optimum location for a receiving array off Canada's west coast for ATOC (Acoustic Thermometry of Ocean Climate). An excellent summary of the original experiment by Baggeroer and Munk can be found elsewhere [6].

This report is organized so as to address the six specific objectives identified in the original contract statement of work. Each of these six objectives had associated with it a detailed task description or "milestone" which was used to guide the research efforts through the course of the entire project. Each section in the following report is preceded by the original milestone description and the ensuing text/figures will describe the degree of success obtained in completing this milestone. The report concludes by summarizing the key findings of this research, discusses how these results will contribute to the scientific study of global warming and suggests a number of areas where additional research is needed to continue this most important work.

2.1 Milestone 1:

Production of a Contractors Report containing the associated non-acoustic data. This report will include information from CFAV Endeavour, CFAV Quest and RV Cory Chouest. The report will be a consistent, systematic presentation of position, environmental, source and receiver status, ocean sound speed, and other pertinent information.

This milestone was successfully completed in April 1993 and the results summarized in a DREP Contractors Report (No. 93-21) [1].

2.2 Milestone 2:

Demonstrated proof that the Doppler correction and time-compression processing has been applied to the complete set of M-sequence signals. The contractor will provide computer files and plotted output of arrival-time vs time spread to demonstrate this milestone.

The Heard Island Feasibility Test took place over a six day period from Jan. 26, 1993 to Jan. 31, 1993 inclusive. Transmissions were made every three hours for about one hour, more or less continuously throughout this period (A gap in the transmissions occurred from 16:00 on Jan. 27th to 09:00 on Jan. 29th, during this period no transmissions were made and the transmitting array was physically recovered aboard the *Cory Chouest*).

The transmissions were of three different types, a continuous single-tone CW transmission at 57 Hz, a pentaline phase-modulated 57 Hz signal that produced 5 major subcarriers at 1.9 Hz separation, and maximal length sequence (M-sequence) transmissions. The 17 M-sequence transmissions consisted of 4 different types varied according to the number of bits in each sequence (and correspondingly in time duration) as follows:

M1	255-bit pseudorandom M sequence (~22.5 sec duration) 57 Hz carrier
M2	511-bit pseudorandom M sequence (~45 sec duration) 57 Hz carrier
M3	1023-bit pseudorandom M sequence (~90 sec duration) 57 Hz carrier
M4	2047-bit pseudorandom M sequence (~180 sec duration) 57 Hz carrier.

These signals were transmitted at regularly scheduled times throughout the entire experiment. JASCO researchers examined 5 of these M-sequences recorded aboard CFAV *Endeavour* off the California coast and 6 M-sequences recorded aboard CFAV *Quest* off the Canadian east coast. The precise times and durations of these recorded signals are available in **[1]**. The findings of this initial investigation are reported elsewhere **[2]**, but a short summary extracted from the INTRODUCTION section of the original paper is reproduced here:

> *In the current work, the interest has been to use correlation techniques with the received M-sequence signals to extract the impulse response of the ocean waveguide. This has been successfully done for the Christmas Island and Acension Island [7,8] receiver locations where the received SNR was very high. At the Canadian receiver in the Pacific the SNR was very low, but a highly capable receiving array was employed with approximately 15 dB of array gain. The net result was an average SNR in a beam of approximately -2 dB/Hz. The received signals in the Atlantic were more variable in strength than those in the Pacific, but on average, the SNR was stronger than in the Pacific. Unfortunately, the Atlantic receiver was far less capable than the Pacific receiver. Only 8 hydrophones were available and the total aperture of the array was just 42 m. The net result was that after beamforming, the mean SNR for both the Pacific and Atlantic receivers was similar, approximately from -2 to -3 dB/Hz.*
>
> *The results of applying the correlation processing to the Canadian data have been less successful than those for the higher SNR data from Christmas and Acension Islands. In fact, we have not been able to directly correlate (i.e., compress) any of the received signals examined so far and obtain a recognizable multipath arrival structure. This failure has prompted a more detailed examination of the modulation scheme and signal processing used with the M-sequences. Our investigation is reported here.*

Thus, in the initial stages of this investigation, the low SNR (Signal to Noise Ratio) found in the raw data was not large enough to permit the direct time-compression of the recorded M-sequences using established constant frequency signal processing methods. In order to ascertain whether there was any possibility of extracting the signal using other methods, a theoretical investigation of the underlying analysis was undertaken. The results of this investigation have been submitted for publication elsewhere **[2]**; however, the conclusions are reproduced below:

> *Spectral analysis has been applied to detect the carrier of the HIFT transmissions and conventional beamforming has provided estimates of the signal energy arrival angle. The analysis of the M-sequence receiver performance has shown that even at the low values of the*

SNR available at the Canadian receiving sites, it should be possible to compress the sequence arrivals and extract the dominant features of the waveguide impulse response at least part of the time. The compression should be a relatively easy problem for the strongest receptions and become more difficult as the weaker receptions are investigated. This statement assumes that the signal frequency is well known. If the signal is sufficiently stable that a mean-doppler frequency removal is sufficient for a time interval extending from one M-sequence period to the the full hour of the pulse transmission, then compression of the data should be possible.

In the HIFT the source was towed; however, good compression results have been obtained at receiving stations with high SNR values. This indicates that the source motion alone was not sufficient to destroy the correlation between the received and replica sequences, provided corrections to the doppler frequency were made on a period-to-period basis.

Both of the Canadian receivers were towed arrays, and thus, subject to changes in motion caused by wave action, temperature and density variations, and unstable propulsion forces. It seems probable that the combined motions of the source and receiver, coupled with the low SNR, which requires longer coherent integration times, and the greater multipath dispersion associated with these very long paths are the likely causes of problems with the pulse compression results of the Canadian HIFT data. We are currently investigating the sensitivity of the processing to changes in Doppler and have developed a method for tracking and removing the Doppler variations for periods of arbitrary length. It is believed that removal of the Doppler frequency changes on a time scale shorter than one period of the M-sequence will allow successful time compression for the stronger than average receptions at the Canadian receivers.

The investigation referred to in the last paragraph of [2] above ultimately led to a second journal publication describing this novel approach [3]. Finally, it was possible to re-examine a limited number of the stronger M-sequence data sets and the results were presented in a third journal article [4]. The net result of this analysis showed that of all twenty-one receptions recorded aboard CFAV ENDEAVOUR, that only two were useful for correlation processing. They were the 511-length M-sequence transmitted at 0900 UTC, 30 January 1993 and the 2047-length M-sequence transmitted at 2100 UTC, 29 January 1993. Figure 1 below is reproduced from [4] and clearly shows the success of the Doppler processing techniques developed in the earlier work.

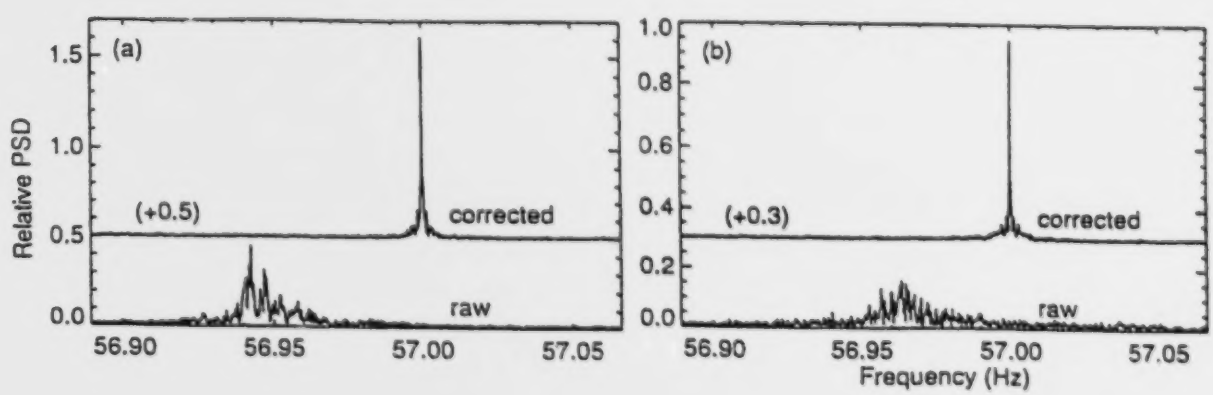

Figure 1. Power spectra before and after dynamic Doppler correction for both the 29 Jan. and 30 Jan. transmission (from [4]).

Fig. 1(a) compares the signal spectra before and after Doppler correction processing for the 29 Jan. transmission, while Fig. 1(b) shows a similar comparison for the 30 Jan. transmission. In both cases there is a dramatic improvement in the spectrum of the measured data. The corrected spectra now clearly show the presence of a single strong spectral component located at the correct carrier frequency of 57 Hz. By comparison, the raw data spectra show low intensity relatively broad spectral regions at frequencies slightly less than the true carrier frequency. This is a dramatic illustration of the improvement that can be obtained by dynamically correcting the Doppler shift.

After correcting for the Doppler variations, the two signals were correlated with replica sequences. Fig. 2 shows the results of the correlation for the 2047-bit M-sequence recorded on Jan. 29th at 21:00 UTC (from **[4]**). This data set was recorded over a 1 hour (3600 s) period and contained 20 repetitions of the 180 second/2047-bit M-sequence. The figure shows that if the time varying Doppler is removed using the phase-tracking techniques described by Schumacher and Heard **[3]** that 17 of 20 possible sequences were detected in this one hour period.

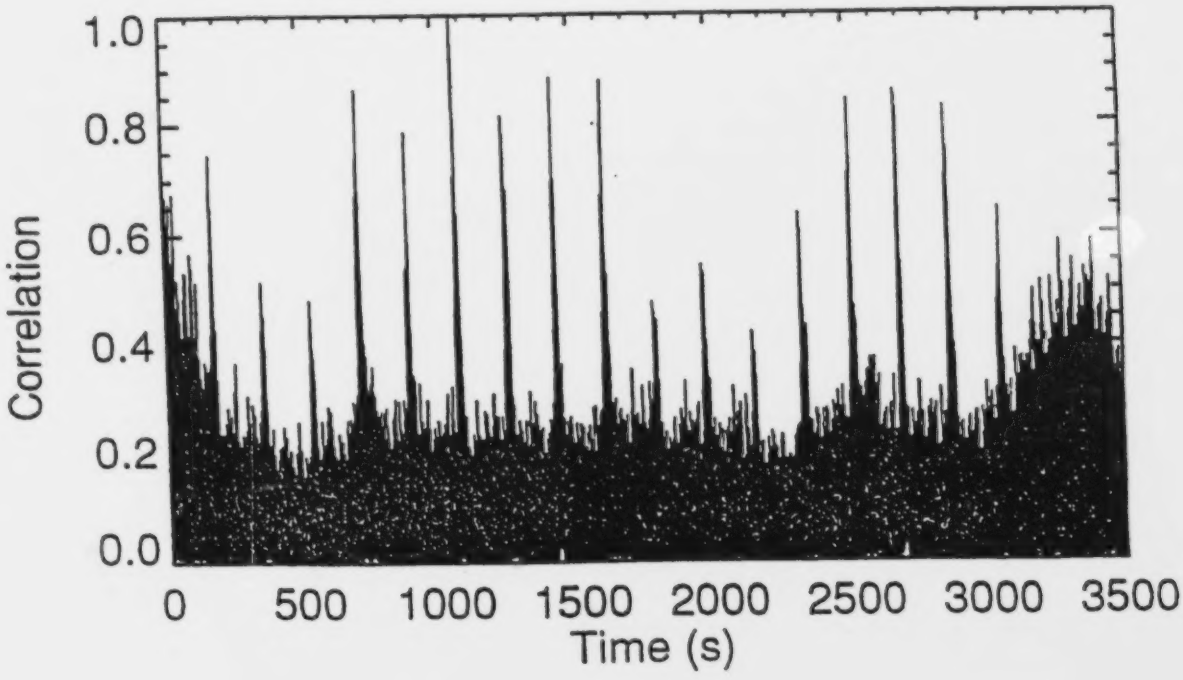

Figure 2. Correlator output with dynamic Doppler correction for the Jan. 29th transmission (from **[4]**).

Fig. 3 shows the results of the correlation for the 511-bit M-sequence recorded on Jan. 30th at 09:00 UTC (from **[4]**). This data set was recorded over a 1 hour (3600s) period and contained 80 repetitions of the 45 second/511-bit M-sequence. The figure shows that once again, if the time varying Doppler is removed using phase-tracking that the M-sequences were detectable, but that poorer results were obtained in this case due to a combination of shorter sequence length and reduced SNR.

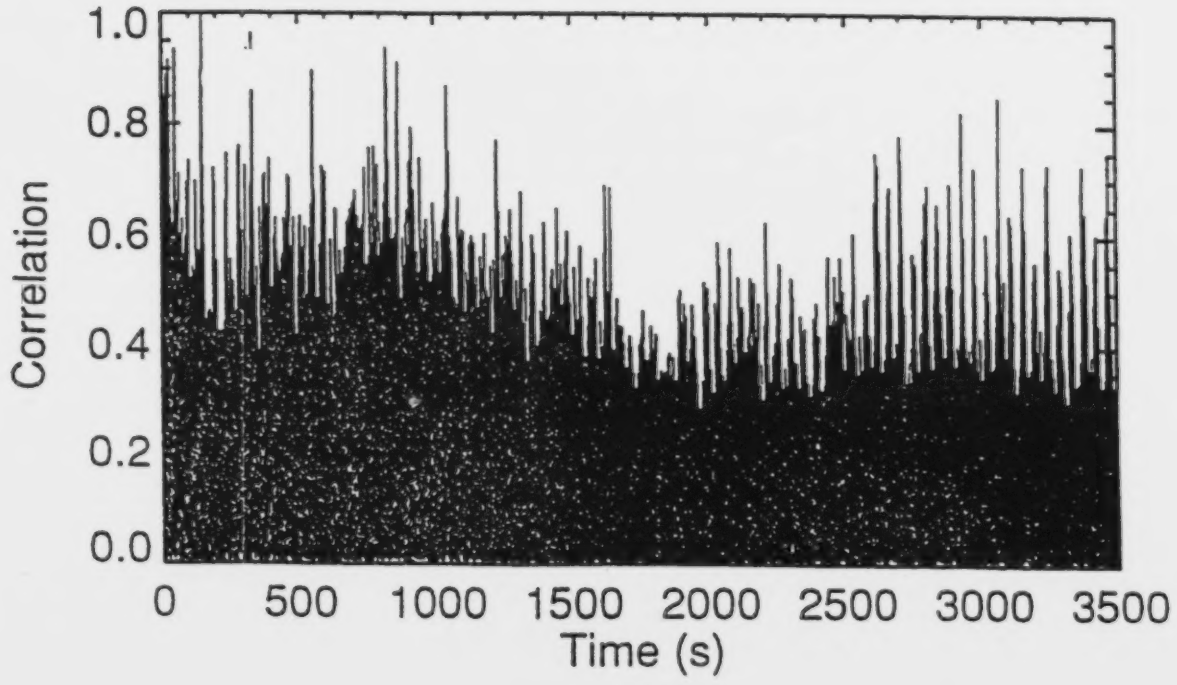

Figure 3. Correlator output with dynamic Doppler correction for the Jan. 30th transmission (from **[4]**).

These arrivals were rearranged to show the intensity of the arrivals as a function of time and time-spread. Figures 4-5 are the *"arrival-time-vs-time spread"* plots referred to in the milestone description at the beginning of this section.

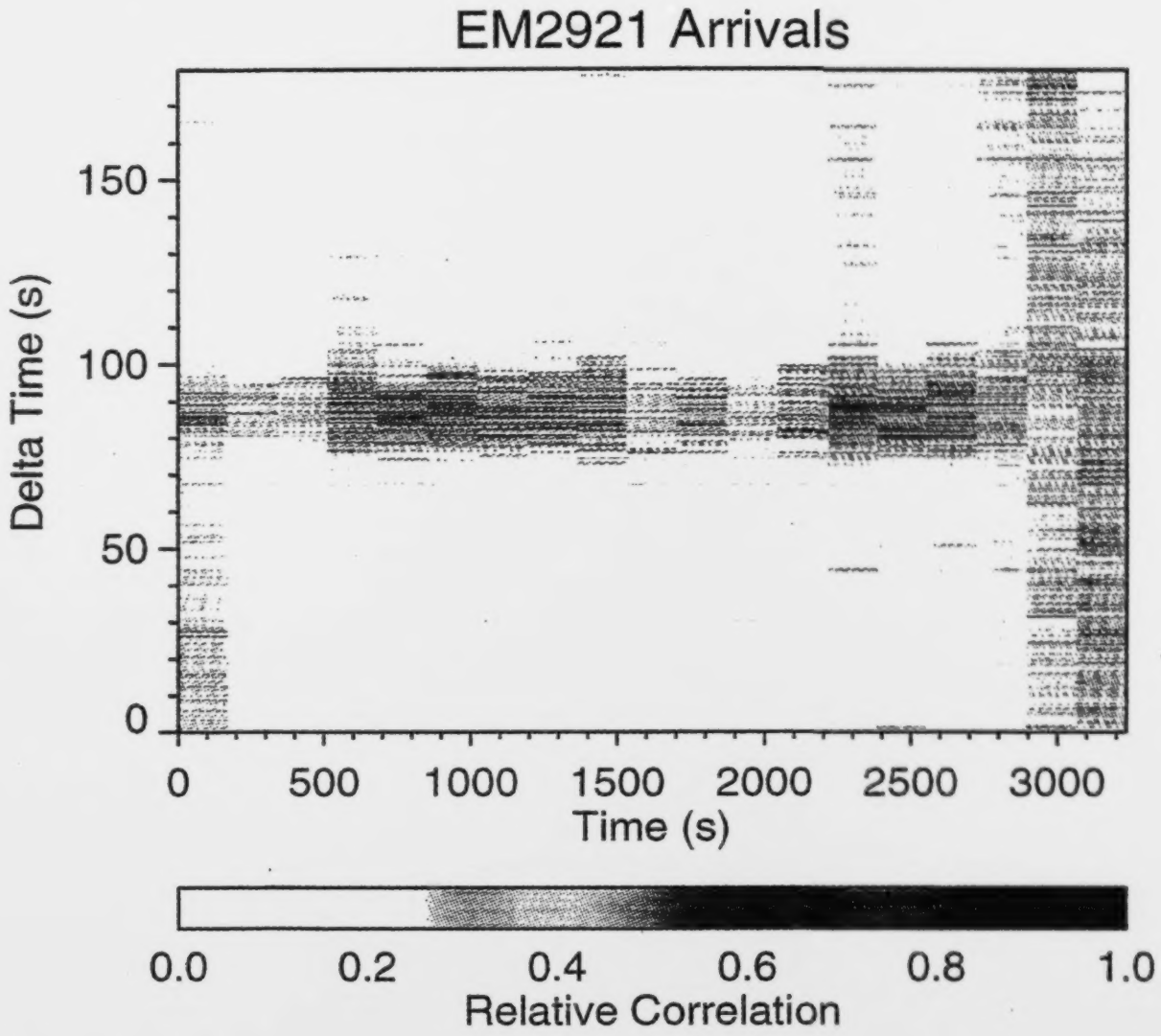

Fig 4. Intensity plot of arrival spread for the 29 Jan. 2100 UTC transmission (from **[4]**).

The horizontal axis of this figure is the elapsed time during the 1-hour transmission period (0-3600 s) and the vertical axis represents the time taken to transmit one complete M-sequence (0-180 s for the 2047-bit M-sequence shown in this figure). The analysis was done so as to ensure that the strongest correlation 'spike' would occur at roughly the 90 s mark, after this, each successive 180 s period was stacked vertically for the full duration of the one hour measurement period.

To understand the arrival structure imagine the simplest possible case where the signal arrives at the receiving array via a single path. After propagating through a completely uniform ocean, the picture would show a high intensity (dark) line at exactly 90 s for the entire one hour measurement period. If the signal arrived at the array via two different paths then one would expect to see two lines, the first at 90 s and the second at 90 s $\pm\triangle$T, where $\triangle$T is the difference in travel time between the paths. By extension, as the number of possible propagation paths increase, the plot would show more and more of these parallel intensity lines distributed about the 90 s arrival line. As the problem increases in complexity due to realistic variability of the ocean medium, non-uniform tow speeds *etc.* each individual path would also be expected to show a variation in arrival time. In our example, for a signal propagating half-way around the world (over 17,000 km in almost 3½ hours) it is reasonable to expect a large number of possible travel paths and a fair degree of variability along each path. This scenario would be expected to cause a spread in the measured arrival times and would result in an arrival-time vs time plot such as that shown in Figure 4 above. It can be seen from this figure that it takes about 28 seconds for the majority of the most significant paths to contribute to the total signal at the array. This appears in the figure as a dark band at around 90 s. If the ocean remained the same day after day, this band would would stay in the same location (90 s); however, if the ocean were to warm up slightly, thus increasing the transmission speed of sound in the ocean, the band would move downward. Heard and Schumacher **[4]** have provided a much more detailed and comprehensive scientific explanation for the observed arrival patterns and compare these results obtained with those measured by other researchers in an earlier journal article.

Figure 5 shows the arrival-time-vs-time plot for the second of the two useable M-sequence data sets. This second set contains the 511-bit M-sequence transmitted on Jan. 30. In this figure the horizontal axis once again represents elapsed time of the one hour signal transmission (3600 s) and the vertical axis represents the time duration of one cycle of the 511-bit M-sequence (45 s). Since the M-sequence is shorter, more complete sequences can be transmitted in the one hour period. The result of this is that the arrival-time-vs-time plot shows 80 repetitions of the M-sequence compared to 20 in Figure 4. As seen in the figure, the arrival structure exhibits once again a spread in arrival times of about 28 seconds. A more detailed explanation is provided in **[4]**.

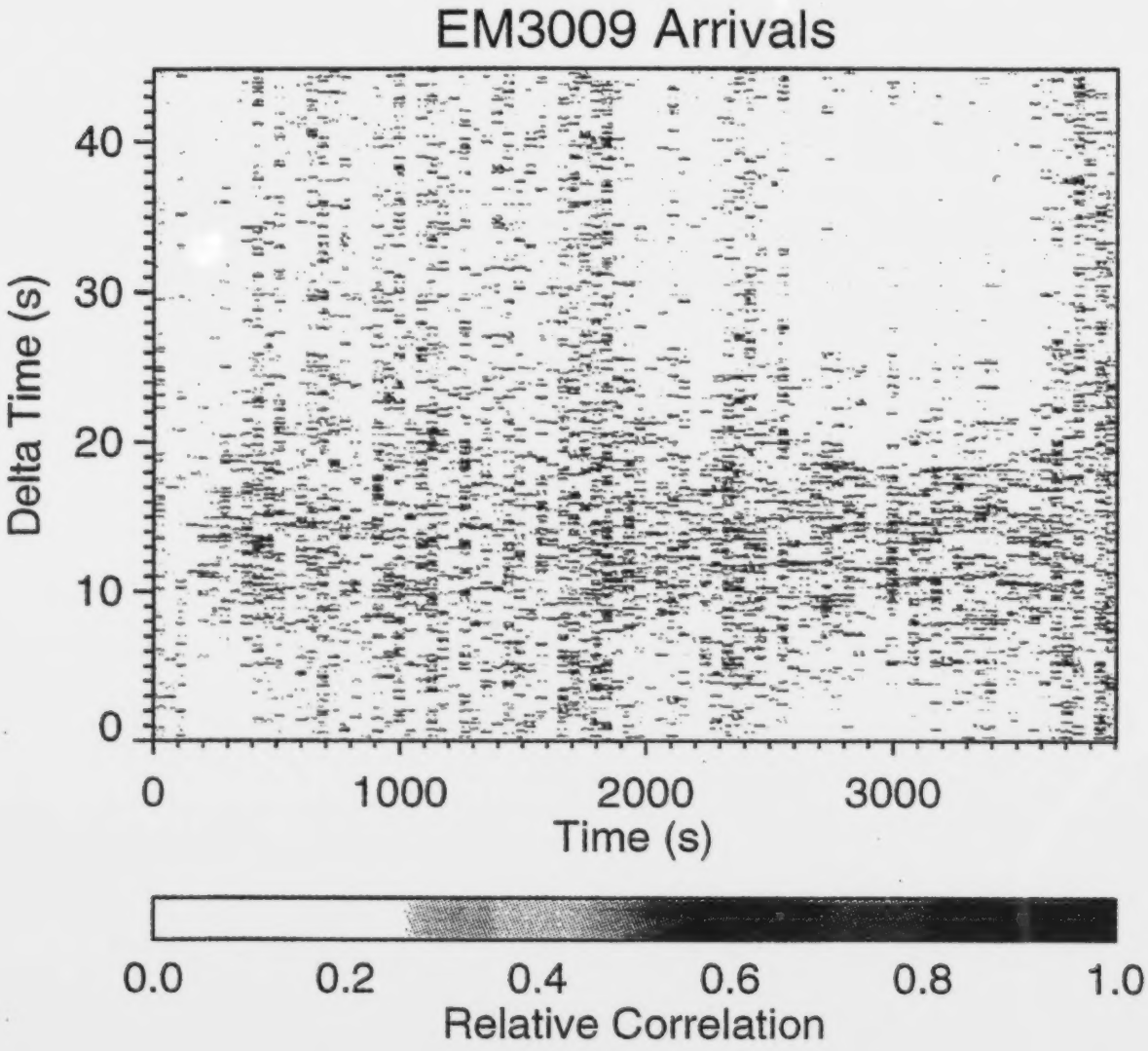

Fig 5. Intensity plot of arrival spread for the 30 Jan. 0900 UTC transmission (from **[4]**).

2.3 Milestone 3:

Demonstrated proof that all signals have been beamformed by conventional means to an angular resolution of several degrees and that selected events have been beamformed to as small an angular resolution as possible with existing hardware and software. The result of this work will be a set of beam time-series data files and frequency-vs-arrival angle plots and data files.

All available signals were beamformed using a time-domain beamformer **[5]** following the spectral analysis methodology described in **[2]** *i.e.*,

The Pacific data were processed into 37 cone shaped beams, uniformly spaced in sin θ, spanning the forward to aft endfire directions. Due to array motion, the strongest arrivals were found to occur on two adjacent beams, which were then averaged to obtain a single time-series used in the spectral analysis. The Atlantic data was processed in a similar fashion, except that 33 beams were computed for the 8 hydrophones and, because of the width of the beams in this case, the averaging of beam time series was unnecessary.

The signals received by the *Endeavour* were beamformed using the 64, 9.525 m spaced mid-frequency hydrophones from the COAMS array. The signals were beamformed from 0-180° into 37 beams using rectagular shading, giving approximately 3.5° resolution in the vicinity of the Heard Island signal. The signals received by the *Quest* were beamformed using 8, 6 m spaced hydrophones. The signals were beamformed from 0-180° into 33 beams and used rectagular shading. The resulting beam time-series for both the Pacific and Atlantic data sets were stored on Exabyte™ tapes using the standard DREP header and file format. A summary of the stored data is given below (Tables 1-2).

Table 1. The beam time-series files for the Pacific data recorded aboard CFAV *Endeavour*.

Filename	Date (1991)	Start time (Z)	Stop time (Z)	Recording Time (min)	Signal Type/ Transmit Time (Z)
EP2915	29 Jan.	18:15	19:30	75	P 29/1500
EM2921	30 Jan.	00:13	01:15	62	M4 29/2100
ECW3000	30 Jan.	03:12	04:27	75	CW 30/0000
EP3003	30 Jan.	06:13	07:28	75	P 30/0300
EM3006	30 Jan.	09:15	10:30	75	M1 30/0600
EM3009	30 Jan.	12:13	13:28	75	M2 30/0900
ECW3018	30 Jan.	15:17	16:32	75	CW 30/1200
EP3015	30 Jan.	18:13	19:28	75	P 30/1500
EM3018	30 Jan.	21:12	22:27	75	M1 30/1800
EM3021	31 Jan.	00:12	01:27	75	M3 30/2100
ECW3100	31 Jan.	03:12	04:27	75	CW 31/0000

Table 2. The beam time-series files for the Atlantic data recorded aboard CFAV *Quest*.

Filename	Date (1991)	Start time (Z)	Stop time (Z)	Recording Time (min)	Signal Type/ Transmit Time (Z)
QM2909	29 Jan.	10:44	12:37	113	M3 29/0900
QCW2912	29 Jan.	14:31	16:02	91	CW 29/1200
QP2915	29 Jan.	18:11	18:55	95	P 29/1500
QM2918	29 Jan.	21:00	22:14	57	M1 29/1800
QM2921	29/30 Jan.	22:50	01:14	120	M4 29/2100
QCW3000	30 Jan.	01:40	04:14	140	CW 30/0000
QP3003	30 Jan.	05:56	06:53	56	P 30/0300
QM3006	30 Jan.	08:56	10:00	61	M1 30/0600
QP3015	30 Jan.	18:22	19:02	28	P 30/1500
QM3018	30 Jan.	21:00	22:11	71	M1 30/1800
QM3021	30/31 Jan.	23:57	00:11	14	M3 30/2100

These data were subsequently examined using frequency-vs-arrival angle plots similar to the one shown in Figure 6.

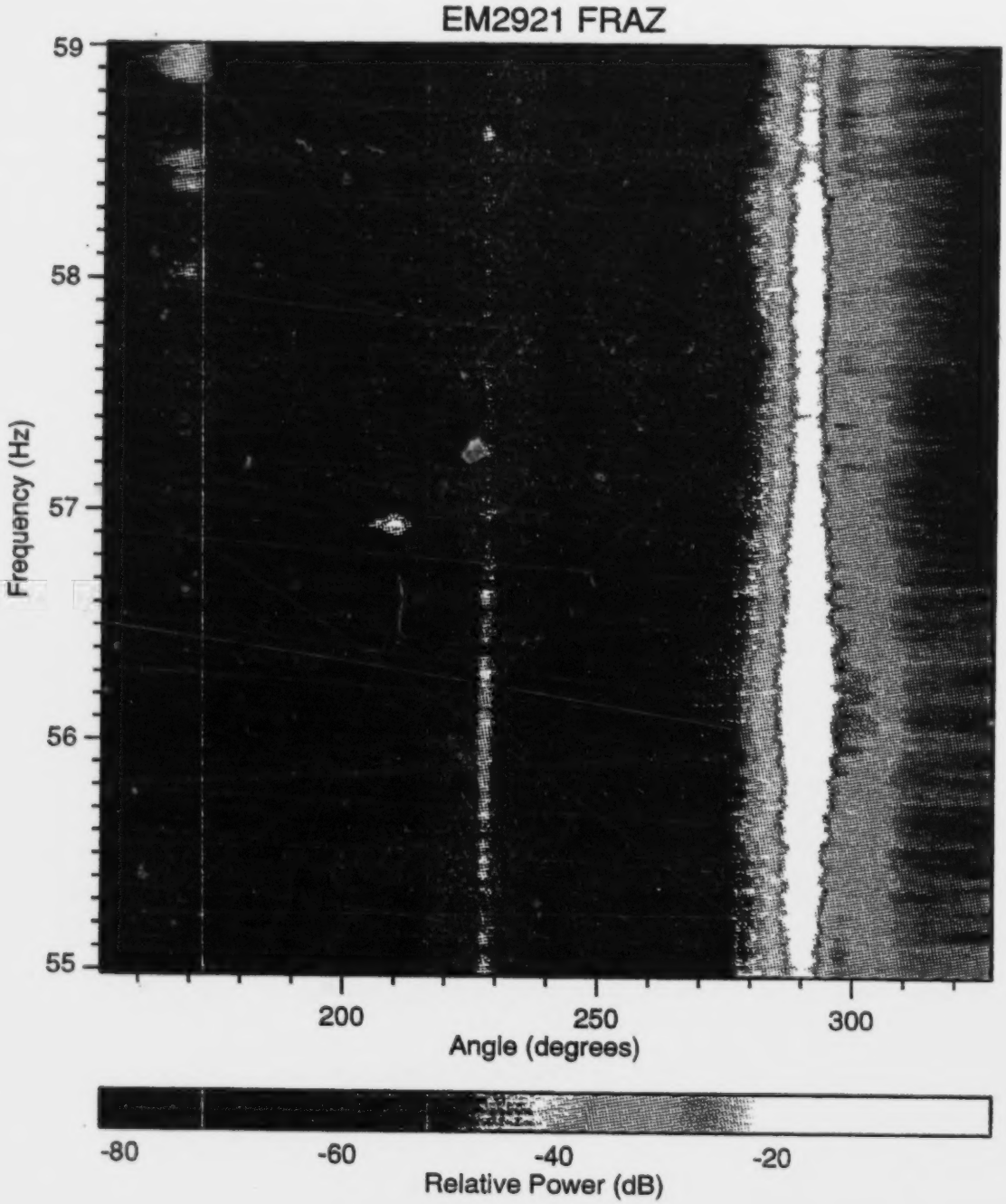

Fig 6. The frequency-vs-arrival angle plot for a portion of the M-sequence transmitted on Jan. 29th at 21:00 UTC and received in the Pacific aboard CFAV *Endeavour*.

Figure 6 shows a typical frequency-vs-arrival angle plot. This plot represents data recorded aboard CFAV *Endeavour* approximately 3 hours and 40 minutes after the start of the Jan. 29th 2100 UTC transmission from Heard Island. Frequency is shown on the vertical axis (55-59 Hz in this example) and the angle of arrival on the horizontal axis. The arrival angle is measured in degrees relative to true North. The figure shows a strong 57 Hz signal arriving from an angle of 212°, or roughly from the south west. This is consistent with the expected direction for incoming signals from Heard Island that are indicated by the red lines of Figure 7. A number of other frequency-vs-arrival angle plots are shown in the next section and in the appendices and most are accompanied by received power-vs-time plots showing the temporal variability of these received signals.

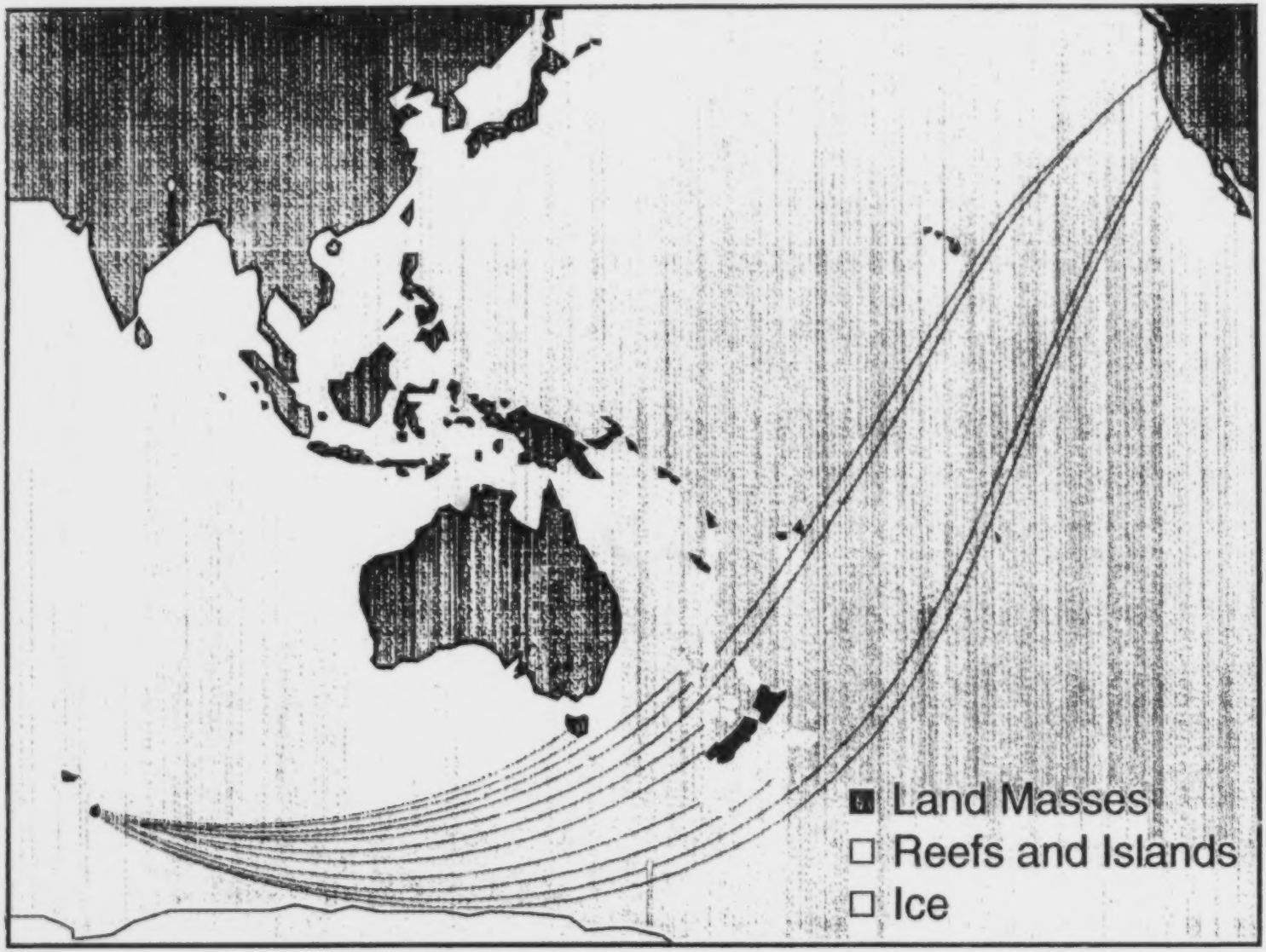

Figure 7. A representation of the possible travel paths of sound transmitted from Heard Island. Note that the majority of the propagated sound is expected to be blocked by ice, land masses and shallow underwater reefs. The data analyzed in this report was propagated along the southernmost paths

2.4 Milestone 4:

A systematic collection of signal amplitude-vs-time, signal phase-vs-time, arrival angle, signal coherence between array elements, Doppler speed-vs-vessel speed, and other pertinent information. This information is to be collected from the initial investigation of arrival structure and spatial and temporal variabilities.

This milestone was associated with the investigation of the spatial and temporal variability of selected events. Figure 8(a) shows the frequency-vs-arrival angle plot for event EM2921, (the event nomenclature refers to the M-sequence event recorded aboard *Endeavour* and transmitted at Heard Island on Jan. 29 at 2100 hours UTC). This plot was for a 24 min data sample taken roughly 17 min into the 1 hour recording period. The 57 Hz HIFT signal can be clearly seen in this figure arriving at an angle of about 212°. Other noise sources appear in the figure as bright vertical bands, for example a loud interfering source can be seen coming into the receiving array at an angle of about 295°.

Figure 8(b) shows the temporal and spatial variability of this signal over the full one hour transmission period. The plot was created by first obtaining an 8192 point (~12 s) FFT using a 50 % overlap. The energy in a 0.5 Hz band surrounding the 57 Hz carrier was then summed to yield a single line representing power-vs-beam angle for that time. This approach was used to provide an estimate of beam power-vs-angle approximately every 6 s. Over the full hour, the 57 Hz HIFT signal appears to vary spatially by about 10°, from ~218° at the start of the reception period to ~208° at the end of the reception period. This apparent variability, however is due to the fact that the arrival angle at the array was calculated using the *average* array heading over the one hour recording period and not the instantaneous array heading. Thus, as the array heading varies over the recording period, it induces an apparent spatial shift in the incoming HIFT signal. In fact, with a fixed receiving array, this signal would be expected to remain stationary in arrival angle over the entire recording period.

The temporal variability of the signal amplitude can also be readily seen in the figure. The signal is first detected at about the 200 s mark (this is most likely the time at which the HIFT signal first arrives at the array). The intensity is relatively high at first and stays more or less uniform until about the 1800 s mark. At this point, the intensity drops markedly for a period of about 300 s, rises again, drops again, rises back to the first level for a period of about 300 s and finally drops off and is lost in the background noise. Figure 9(a) shows this in more detail as an amplitude-vs-time plot. The variability of the phase over this period is shown in Fig. 9(b). Figures 10-11 show another example of the observed signal variability, in this case for event EP3003, the pentaline transmission of Jan 30, at 0300 UTC. A systematic collection of frequency-vs-arrival angle, beam power-vs-time and other plots are included in appendices A and B for the CFAV *Endeavour* and the CFAV *Quest* respectively.

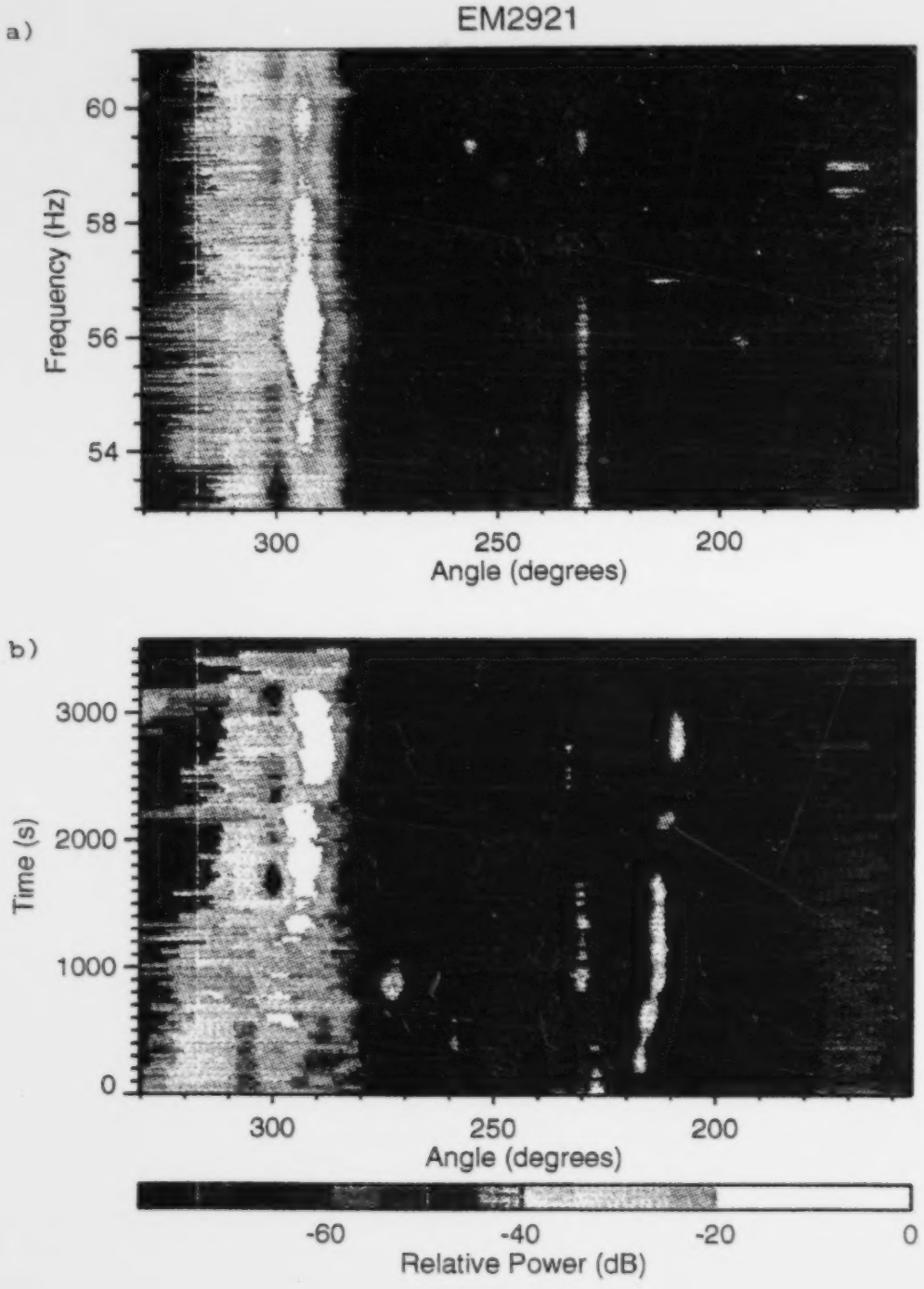

Figure 8. (a) The frequency-vs-arrival angle of the M-sequence transmitted Jan. 29 at 2100 UTC and (b) the beam power-vs-time plot showing the temporal variability of this signal.

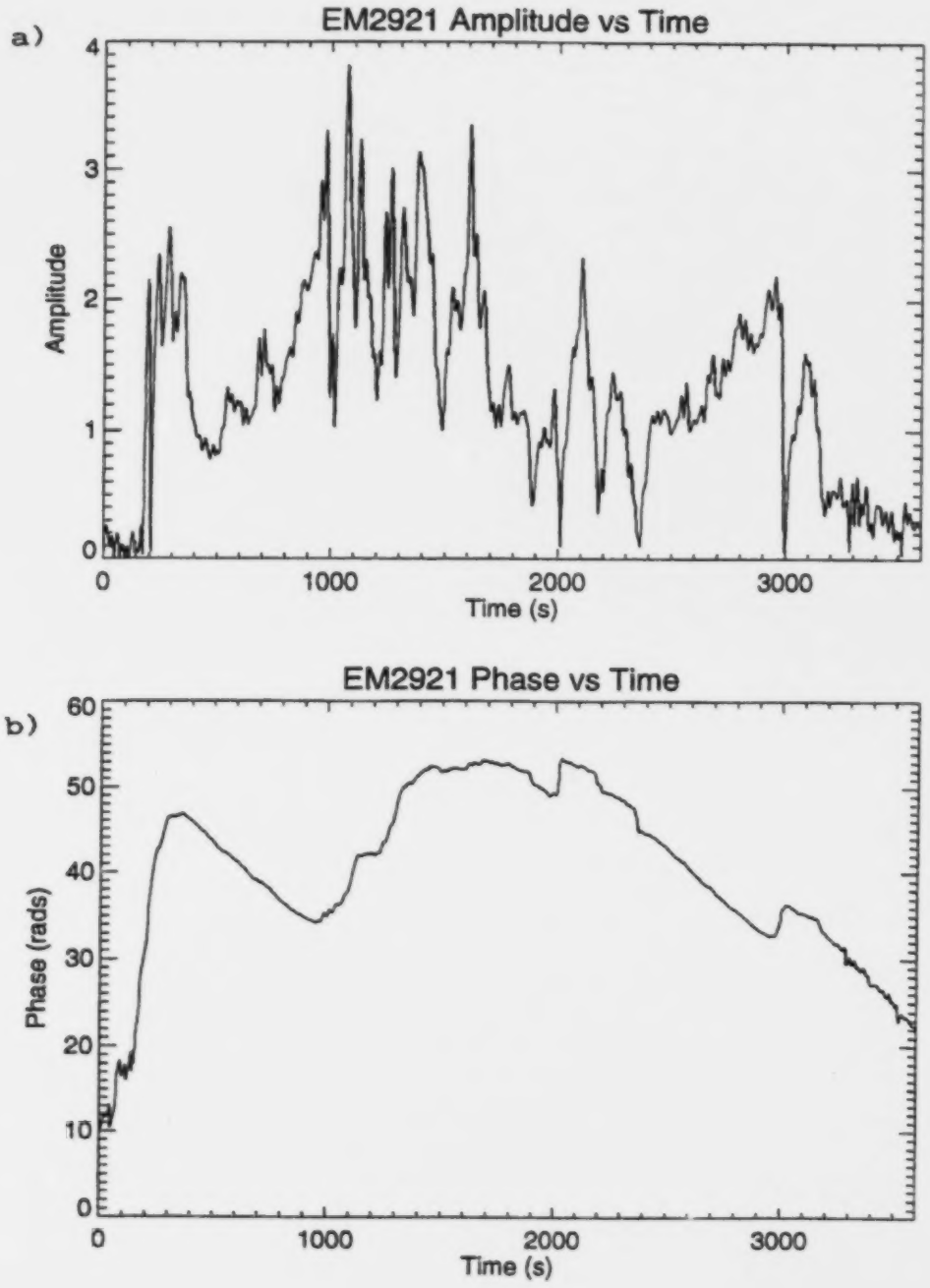

Figure 9. (a) The amplitude-vs-time of the M-sequence transmitted Jan. 29 at 2100 UTC and (b) the phase-vs-time plot showing the temporal variability of this signal.

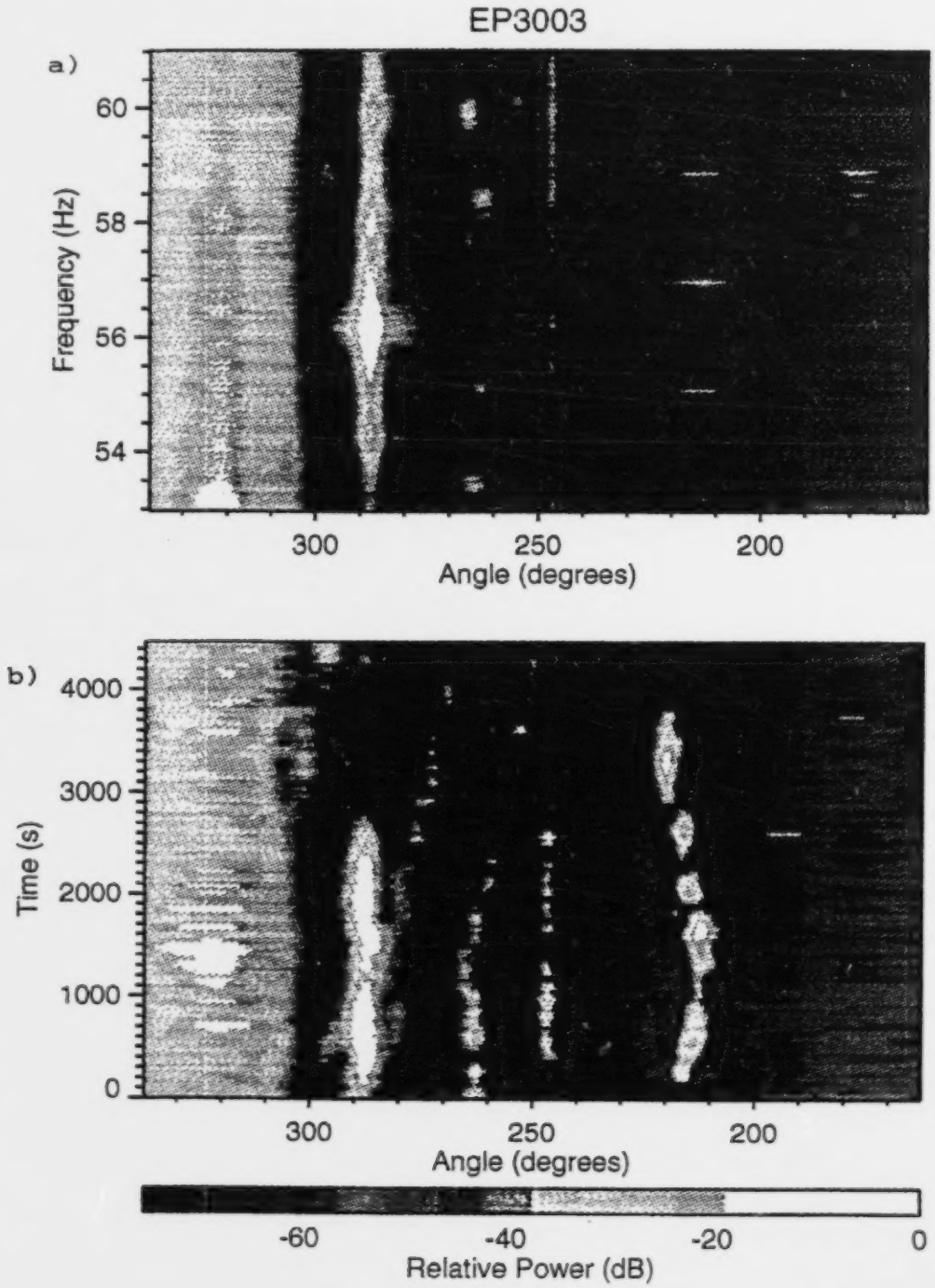

Figure 10. (a) The frequency-vs-arrival angle of the pentaline signal transmitted Jan. 30 at 0300 UTC and (b) the beam power-vs-time plot showing the temporal variability of this signal.

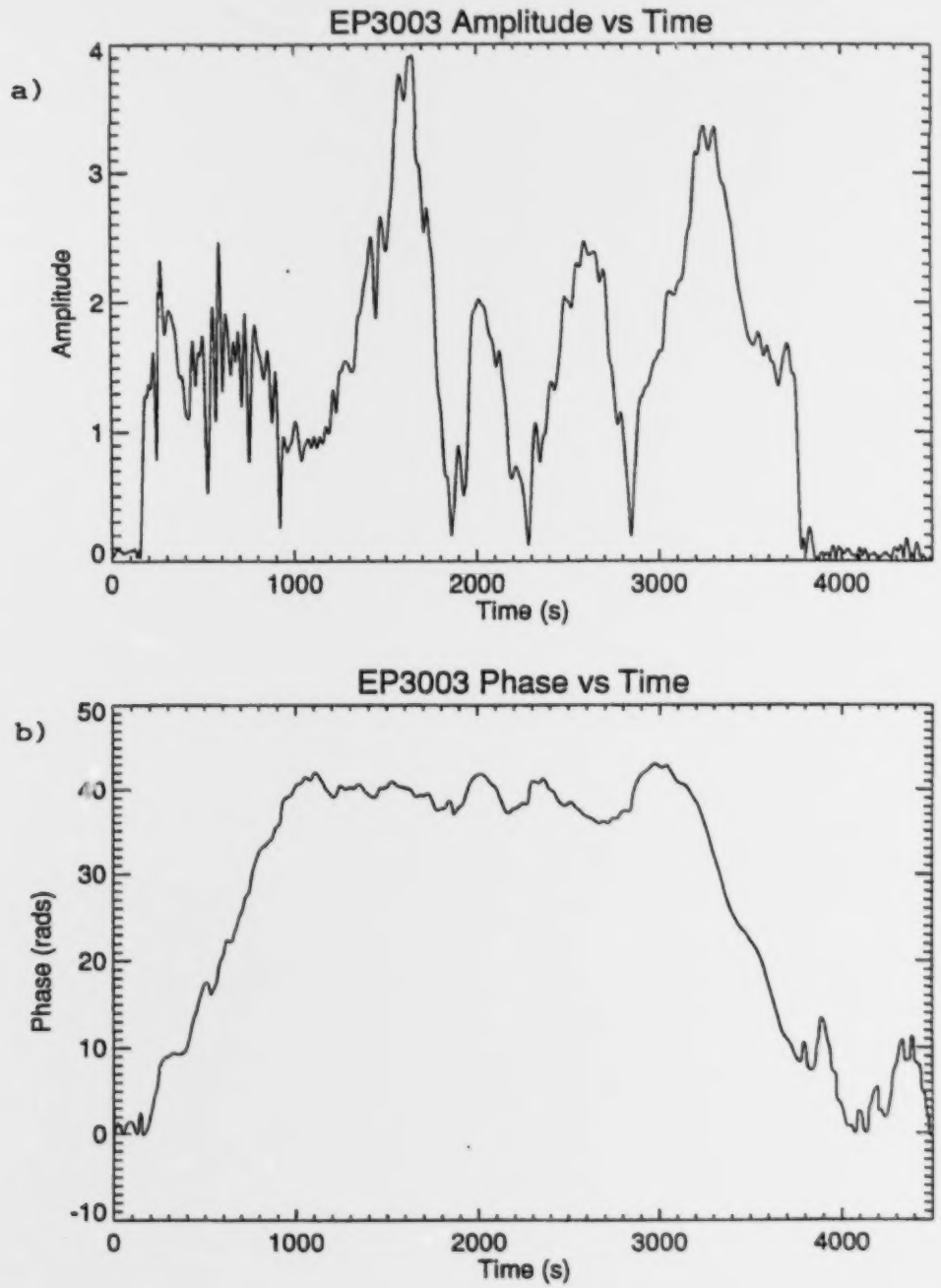

Figure 11. (a) The amplitude-vs-time of the pentaline signal transmitted Jan. 30 at 0300 UTC and (b) the phase-vs-time plot showing the temporal variability of this signal.

2.5 Milestone 5:

Production of a Contractors Report on the site-selection, array definition, and performance of a receiving array that could function as part of the Northern Pacific network.

This work is complete and is available as a DREP Contractors Report (No. 94-63) by J.A. Scrimger and D.M. Henderson entitled "*Considerations for Optimal Siting of Receiving Arrays off Canada's West Coast for ATOC (Acoustic Thermometry of Ocean Climate)* **[5].**

2.6 Milestone 6:

Production of the final Contractor's Report. This comprehensive document will contain all pertinent information derived from this study.

(This report).

3. Conclusions

A number of important results were found in the course of this research work which will be of considerable interest to the scientific community involved in the acoustic research work associated with measurement of global warming.

1. It was found that signals propagated over very long distances (≈17,300 km in the Pacific and ≈16,700 km in the Atlantic) could be readily detected by the Canadian receiving arrays aboard CFAV *Endeavour* and CFAV *Quest*. The preliminary results were first reported by Chapman and Heard **[10]** for the Pacific data and by Fraser and Morash **[11]** for the Atlantic data.

2. It was discovered that even though the 57 Hz carrier frequency was clearly present in most of the available acoustic data sets, that this was not sufficient to ensure that the encoded M-sequences could be extracted from the raw data. This finding ran contrary to our initial expectations and led to a more detailed examination of the relationships between SNR and M-sequence extraction. The results of this study **[2]** led to expressions detailing the relationships between SNR and the probability of signal detection for M-sequence processing. These results will be extremely useful to future researchers in the planning of similar experiments.

3. Examination of the two strongest acoustic data sets showed that the relative motion of the source and receiving arrays had a significant negative impact on the ability to extract the M-sequence from within the received raw data. It was determined that the relative motion induced a Doppler frequency shift which lowered and 'smeared' the expected carrier frequency from a single strong tone at exactly 57 Hz to a broader spectral 'hump' which wandered about 57 Hz. A second investigation was undertaken to examine the

effects of Doppler on M-sequence extraction and led to the development of a method to correct for these observed motion effects. This method was applied to the entire data set however only two yielded useful results.

4. A*rrival time-vs-time* plots were made for two events, the first was the Jan. 29, 21:00 UTC 2047-bit M-sequence transmission and the second was the Jan. 30, 09:00 UTC 511-bit M-sequence transmission. These plots show that the arrival times are distributed more or less uniformly with a spread of about 28 s as reported in **[4]** *i.e.*

"The distribution of energy in the arrival patterns for both transmissions is almost symmetric. This result was somewhat surprising, since a sofar type of arrival was expected, where most of the energy would have arrived toward the end of the arrival structure. One possible explanation is that the higher order modes are simply not present and that the arrival structure is due entirely to a few low-order modes".

Heard and Schumacher go on to examine the relationship between signal propagation range and the spread in observed arrival time and report that it appears to be linear.

5. The study has shown that the acoustic technique described in this (and other) reports can provide a mechanism for measuring global oceanic temperature change. A sufficiently large fluctuation in water temperature would show a corresponding shift in the arrival time distribution and thus the technique can be used as a sort of global thermometer. The next question is really a question of sensitivity, *i.e.* is a thermometer of this type sufficiently sensitive that it can be used to measure the small temperature variations associated with global warming? The answers to this may be forthcoming as a result of ongoing research currently underway with the ATOC (Acoustic Thermometry of Ocean Climate) and GAMOT (Global Acoustic Monitoring of Ocean Temperature) programmes.

References

[1] P. Scrimger, R. Racca, I.Schumacher, D. Henderson, G. Heard, and I.A. Fraser, "A summary of non-acoustic data from the Heard Island Feasibility Test pertaining to the Canadian receiving stations", Defence Research Establishment Pacific Contractors Report, DREP CR/93-21, JASCO Research Ltd.,Sidney, B.C., Canada, April (1993)

[2] G.J. Heard and I. Schumacher, "Correlation processing of the Heard Island Feasibility Test data", submitted to J. Acoust. Soc. Am. (August 18, 1993).

[3] I. Schumacher and G.J. Heard, "Removal of time varying Doppler using phase tracking and interpolation with application to ocean warming measurements", accepted for publication in J. Acoust. Soc. Am. (1993).

[4] G.J. Heard and I. Schumacher, "Time compression of M-sequence transmissions in a very long waveguide with a moving source and receiver", submitted to J. Acoust. Soc. Am. (December 1, 1993).

[5] J.A. Scrimger, D.M. Henderson, "Considerations for optimal siting of receiving arrays off Canada's west coast for ATOC (Acoustic Thermometry of Ocean Climate)", Defence Research Establishment Pacific Contractors Report, DREP CR/94-63, JASCO Research Ltd., Sidney, B.C., Canada, April (1994)

[6] A. Baggeroer and W. Munk, "The Heard Island Feasibility Test", Physics Today, **45**(9), 22-30, (1992)

[7] T.G. Birdsall, M.A. Dzieciuch, and K. Metzger Jr., "Heard Island Feasibility Test signal processing first results", informal publication from the Communications and Signal Processing Laboratory of the EECS Dept., University of Michigan, Ann Arbor, Michigan 48109-2122, May (1991)

[8] A.M.G. Forbes, "Ocean Acoustic Thermometry - the Heard Island Feasibility Test, 1991", Acoustics Australia, **20**(3), 87-90, December (1992)

[9] R. Racca and I. Schumacher, "FLATDAN Beamformer enhancements and testing,", Defence Research Establishment Pacific Contractors Report, DREP CR/92-27, JASCO Research Ltd., Sidney, B.C., Canada, July (1992)

[10] G.J. Heard and N.R. Chapman, "Heard Island Feasibility Trial: Analysis of the Pacific path data obtained with a horizontal line array,"accepted for publication in the Special issue of J. Acoust. Soc. Am. on the HIFT, (February, 1992).

[11] I.A. Fraser and P.D. Morash, "Observation of the Heard Island signals near the Gulf Stream," accepted for publication in the Special issue of J. Acoust. Soc. Am. on the HIFT, March (1992).

Appendix A

Additional Frequency-vs-Arrival Angle

and

Beam Power-vs-Time

Plots

from CFAV *Endeavour*

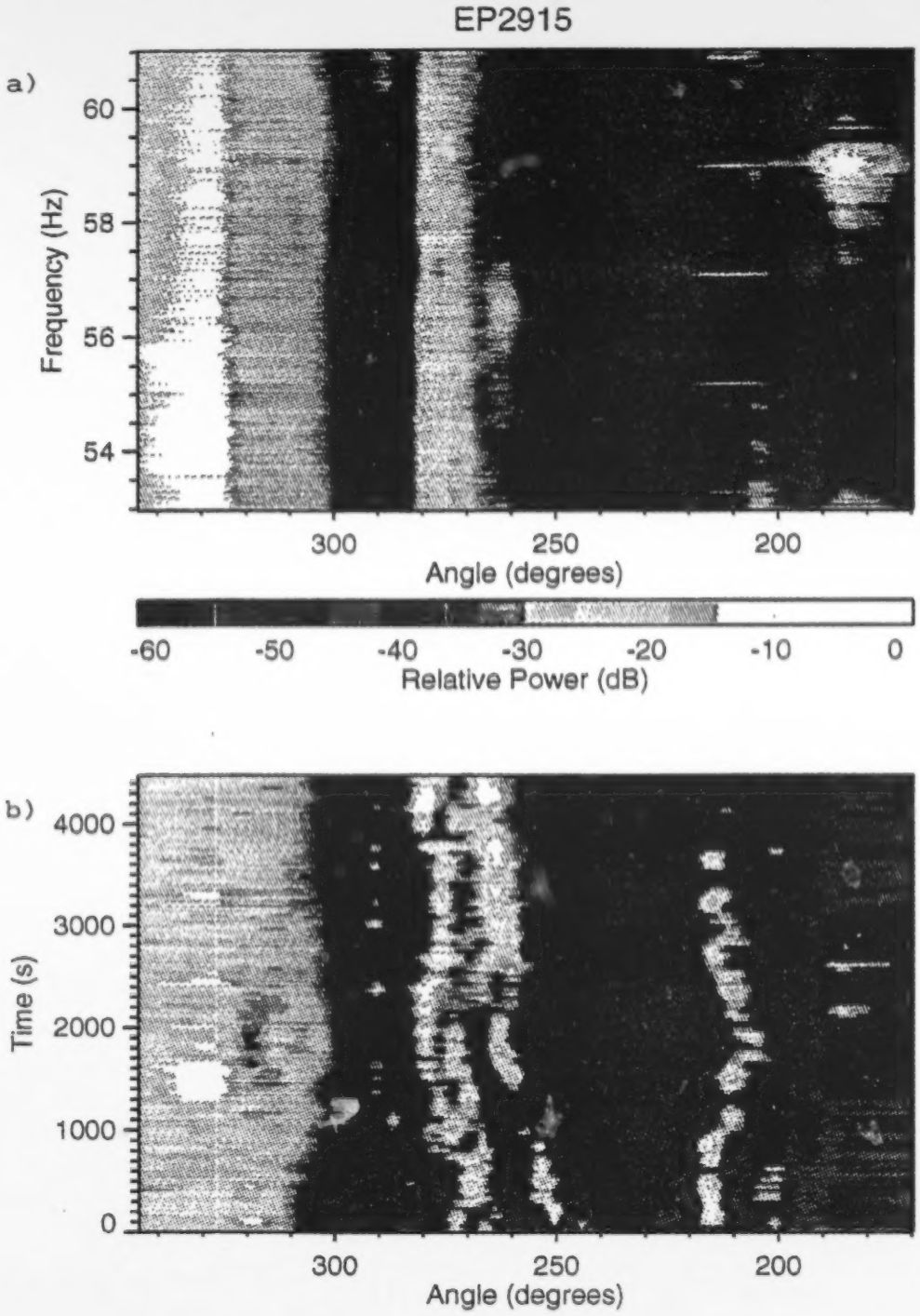

Figure A1. (a) The frequency-vs-arrival angle of the pentaline signal transmitted Jan. 29 at 1500 UTC and (b) the beam power-vs-time plot showing the temporal variability of this signal.

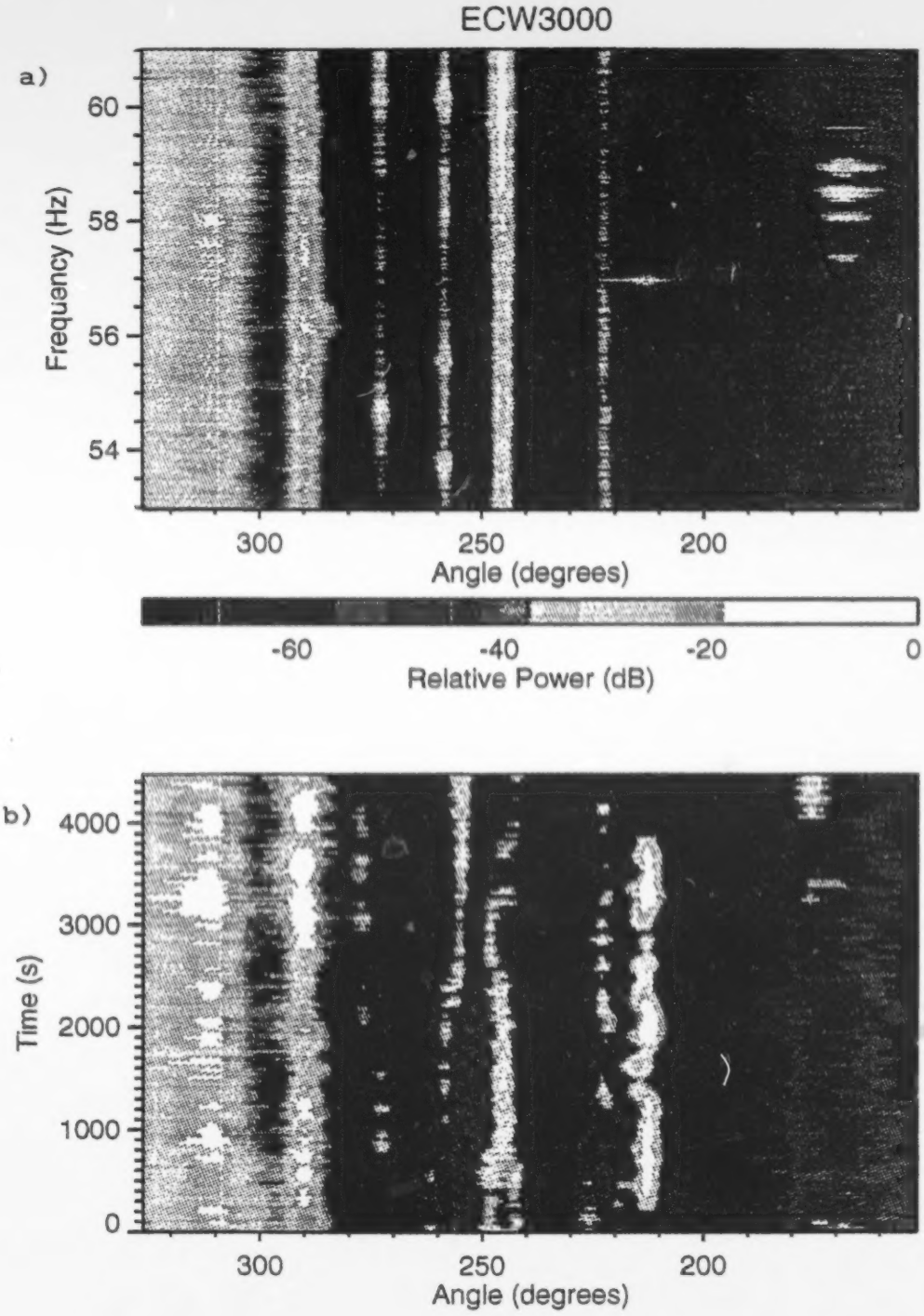

Figure A2. (a) The frequency-vs-arrival angle of the CW signal transmitted Jan. 30 at 0000 UTC and (b) the beam power-vs-time plot showing the temporal variability of this signal.

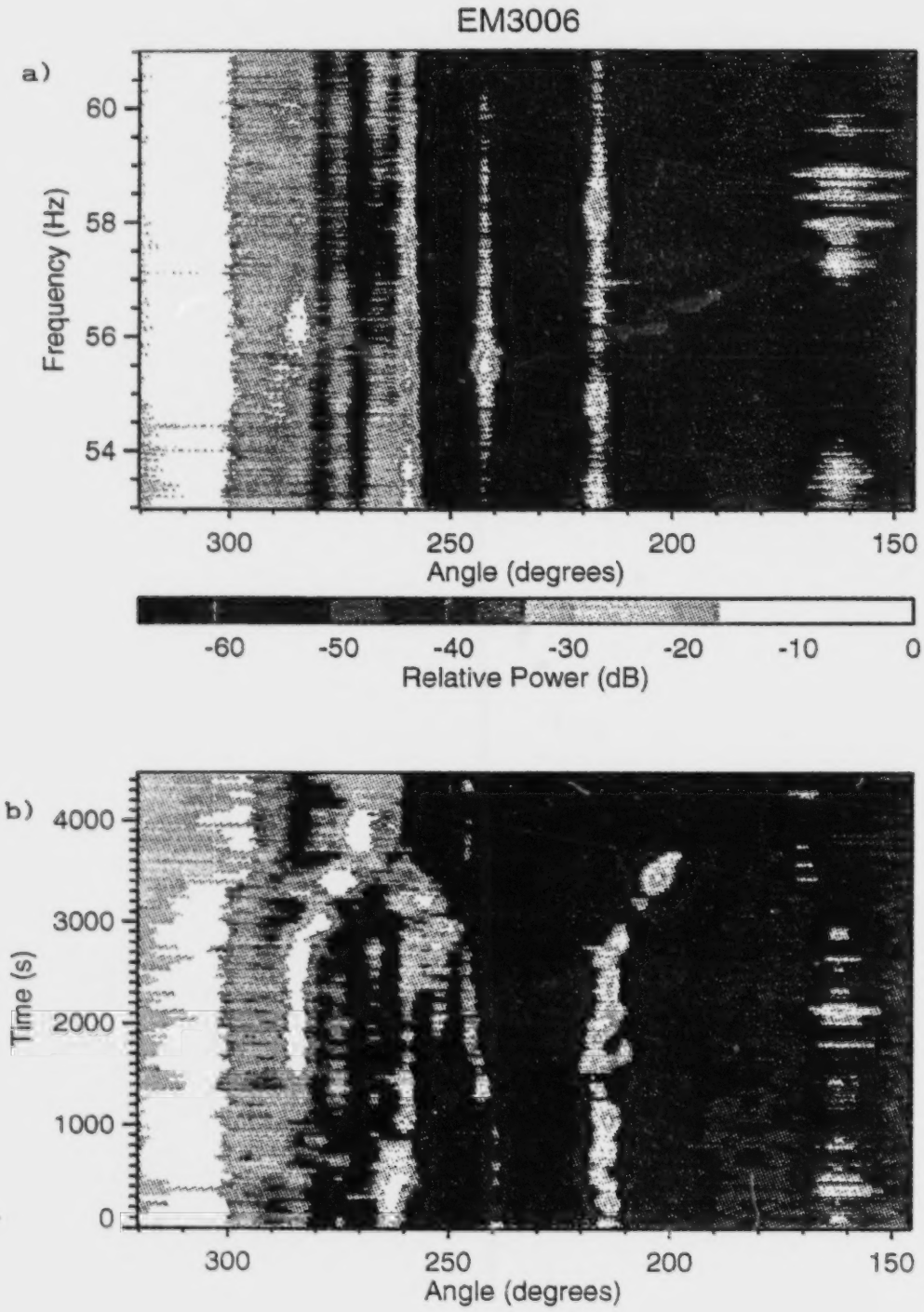

Figure A3. (a) The frequency-vs-arrival angle of the M-sequence transmitted Jan. 30 at 0600 UTC and (b) the beam power-vs-time plot showing the temporal variability of this signal.

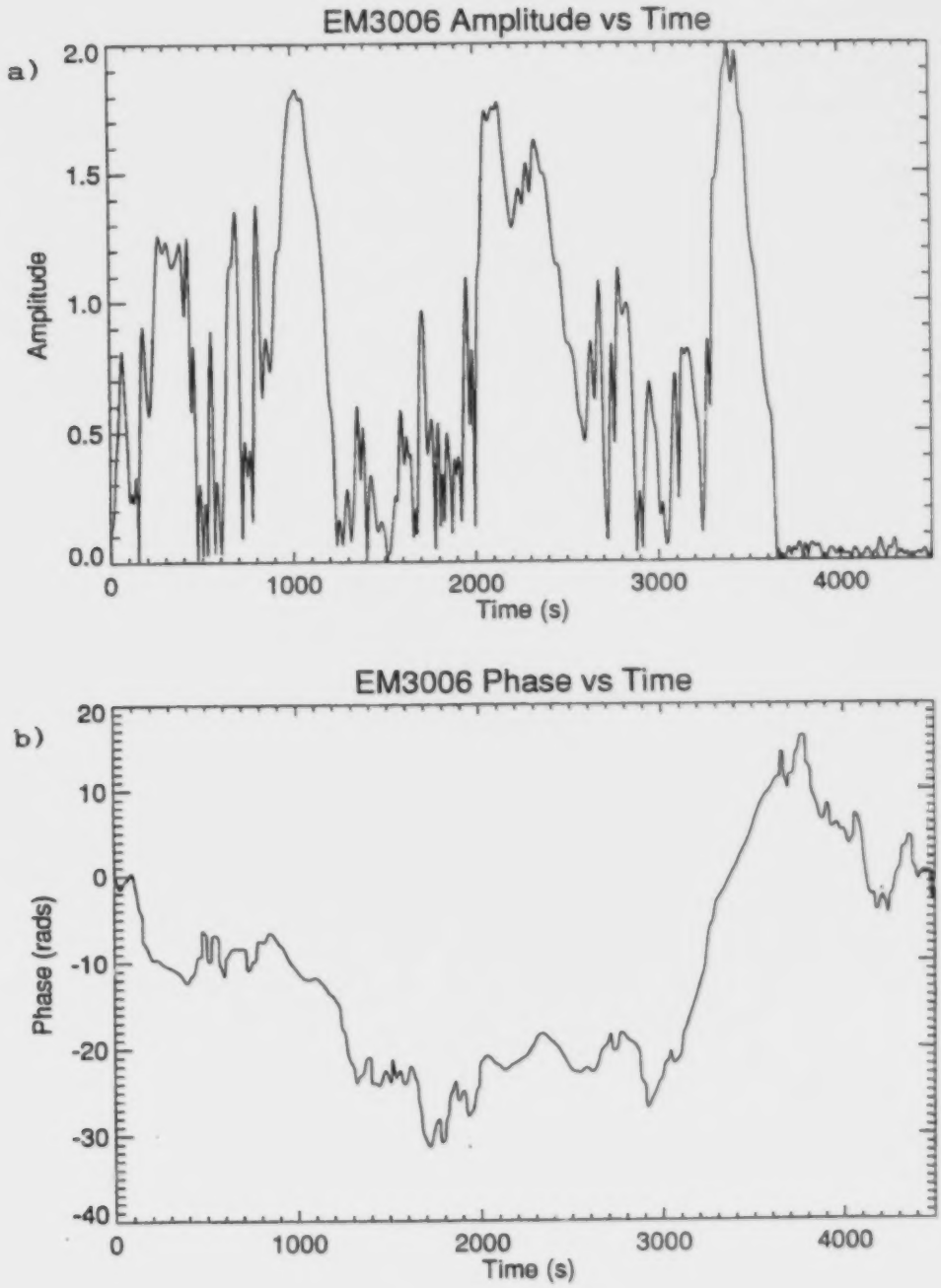

Figure A4. (a) The amplitude-vs-time of the M-sequence transmitted Jan. 30 at 0600 UTC and (b) the phase-vs-time plot showing the temporal variability of this signal.

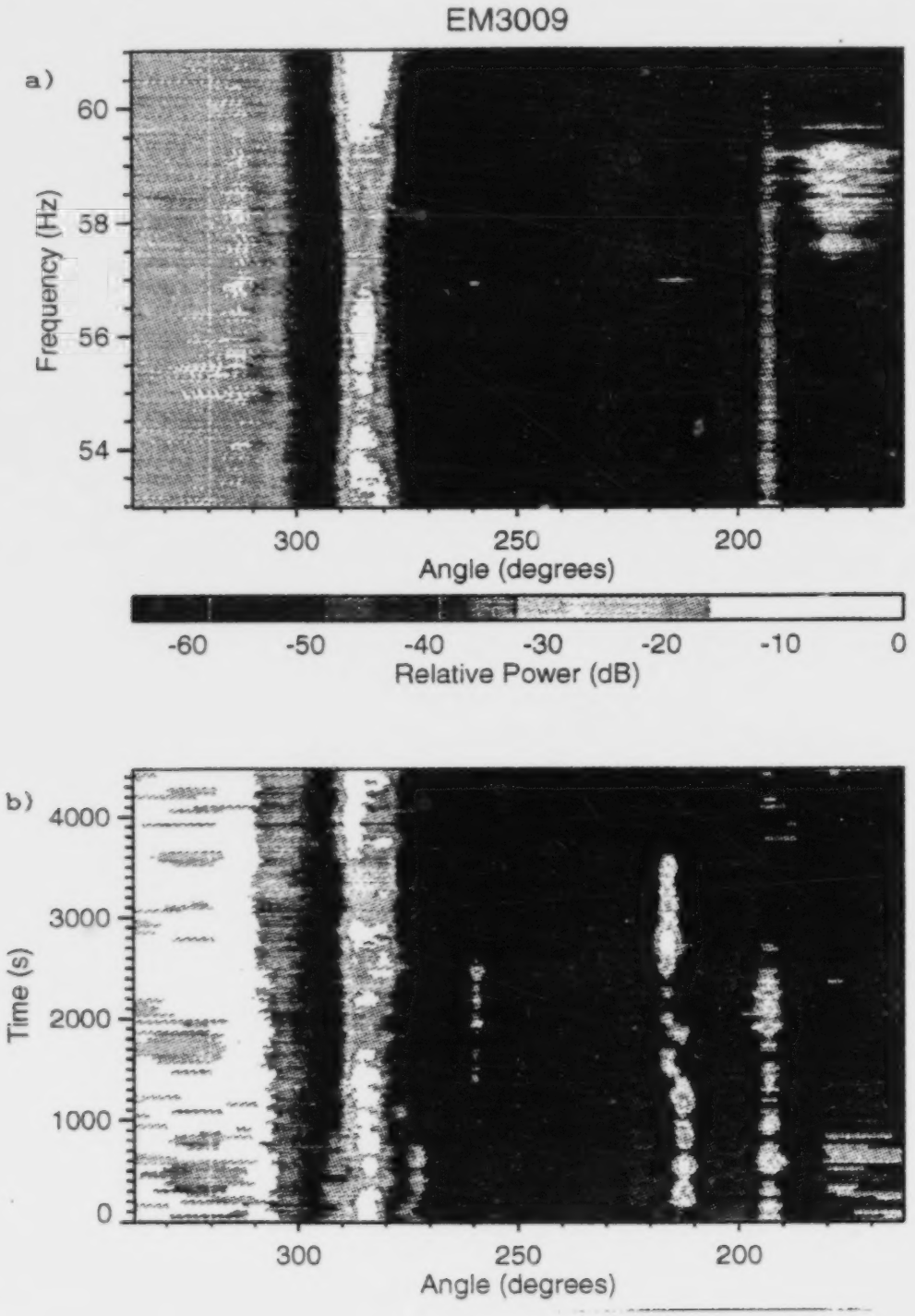

Figure A5. (a) The frequency-vs-arrival angle of the M-sequence signal transmitted Jan. 30 at 0900 UTC and (b) the beam power-vs-time plot showing the temporal variability of this signal.

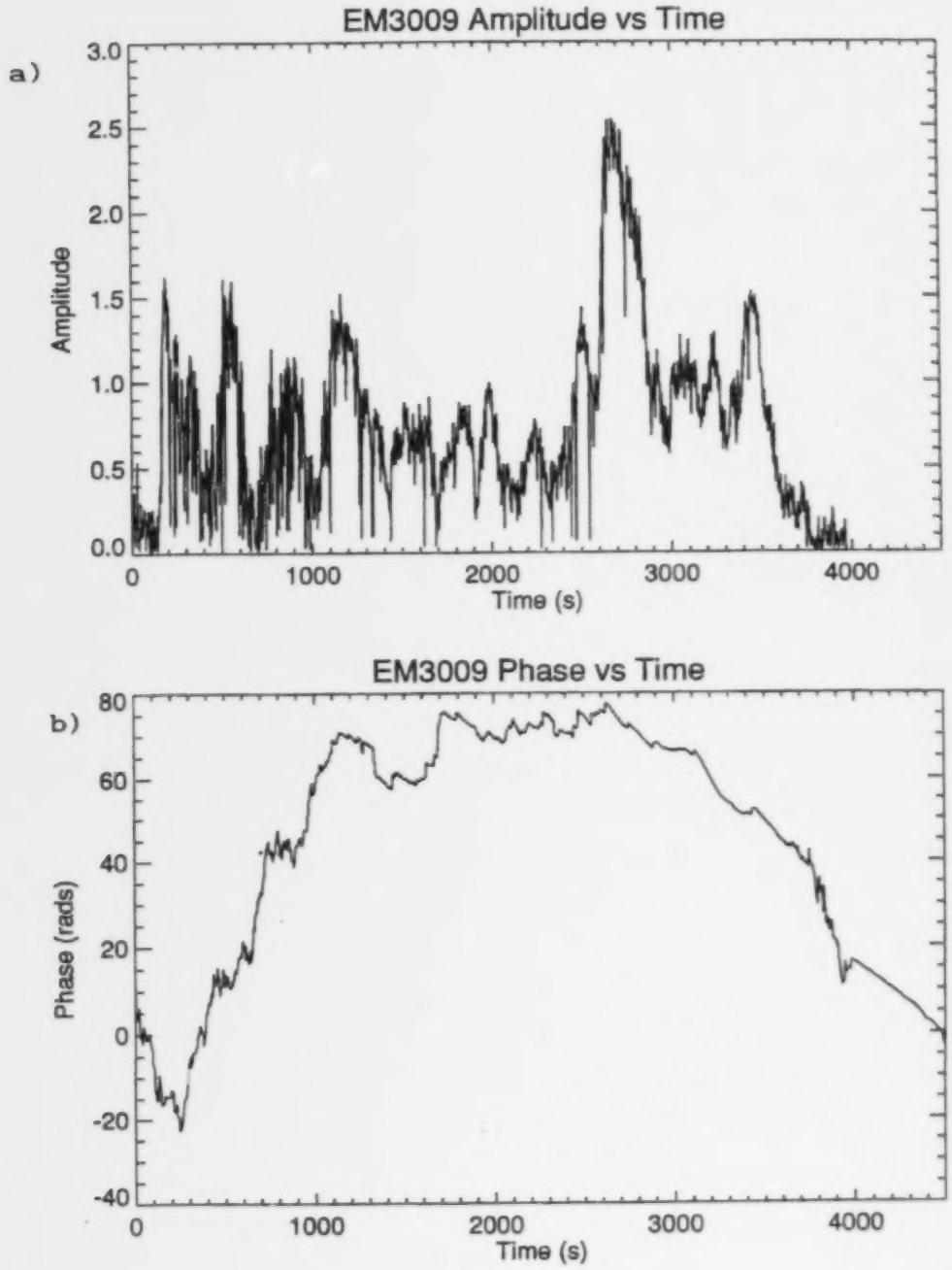

Figure A6. (a) The amplitude-vs-time of the M-sequence transmitted Jan. 30 at 0900 UTC and (b) the phase-vs-time plot showing the temporal variability of this signal.

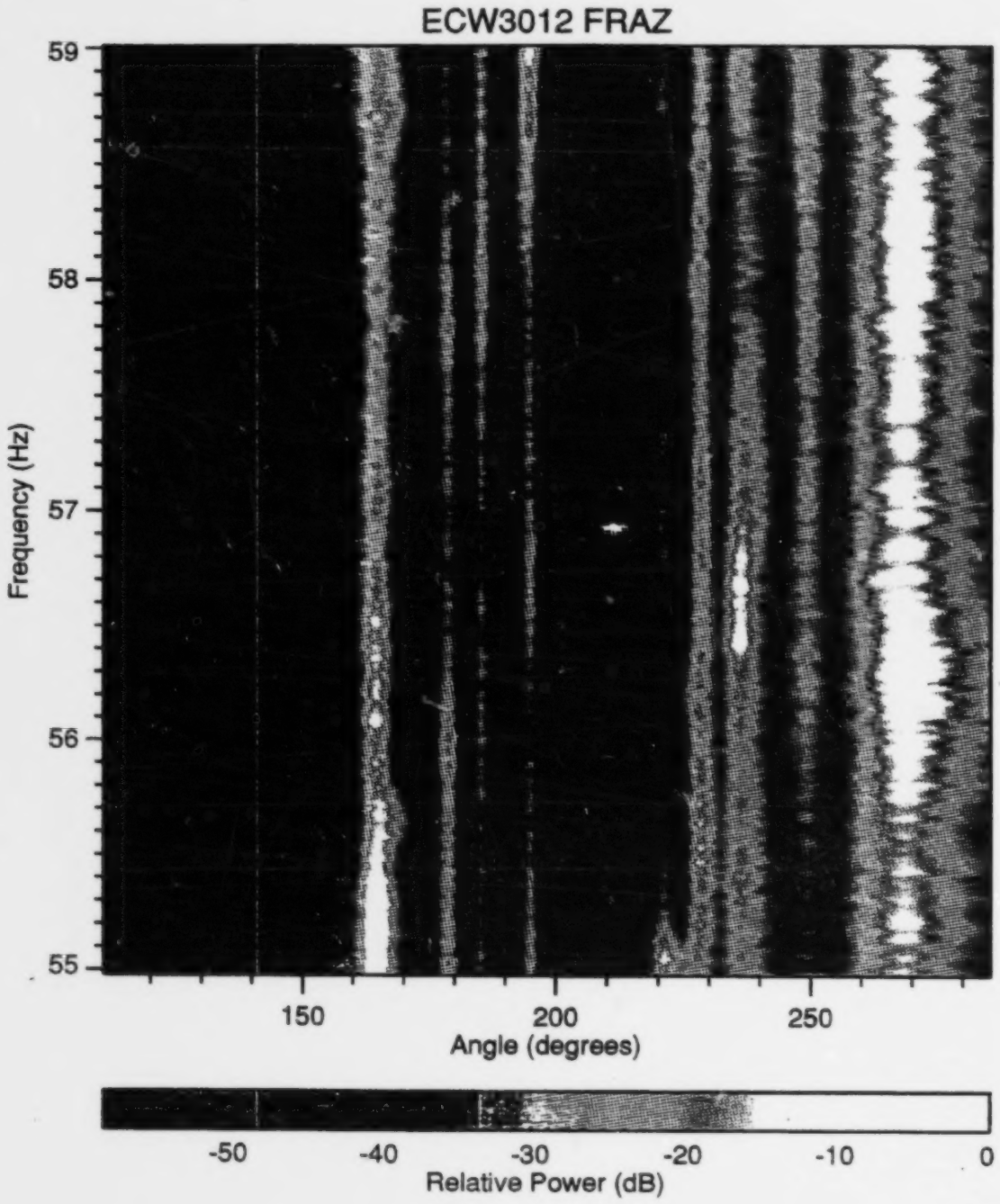

Figure A7. The frequency-vs-arrival angle of the CW signal transmitted Jan. 30 at 1200 UTC.

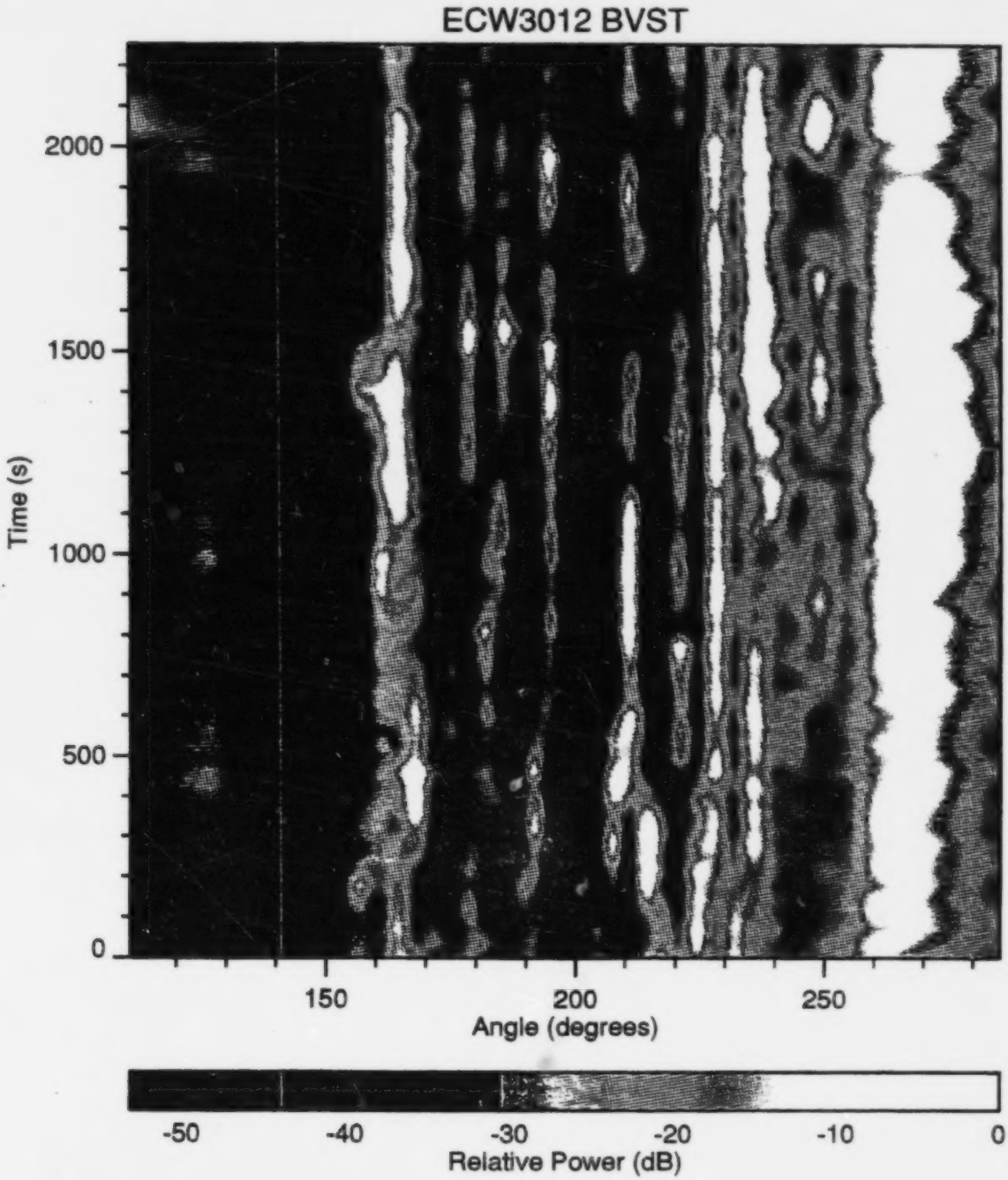

Figure A8. The beam power-vs-time plot of the CW signal transmitted Jan. 30 at 1200 UTC.

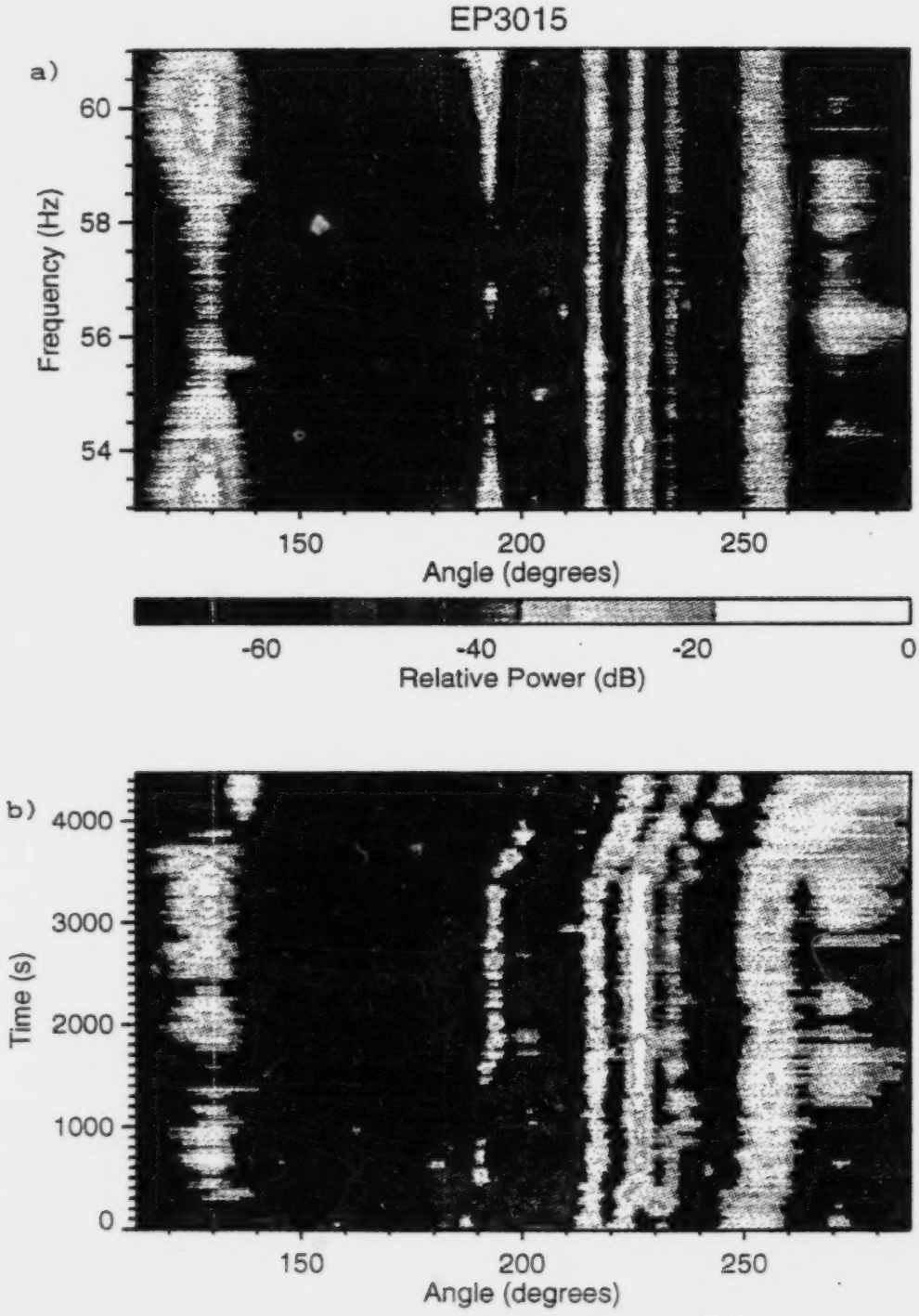

Figure A9. (a) The frequency-vs-arrival angle of the pentaline signal transmitted Jan. 30 at 1500 UTC. The signal is incoming at an arrival angle of about 228°. Figure A9(b) shows the beam power-vs-time plot showing the temporal variability of the 57 Hz signal.

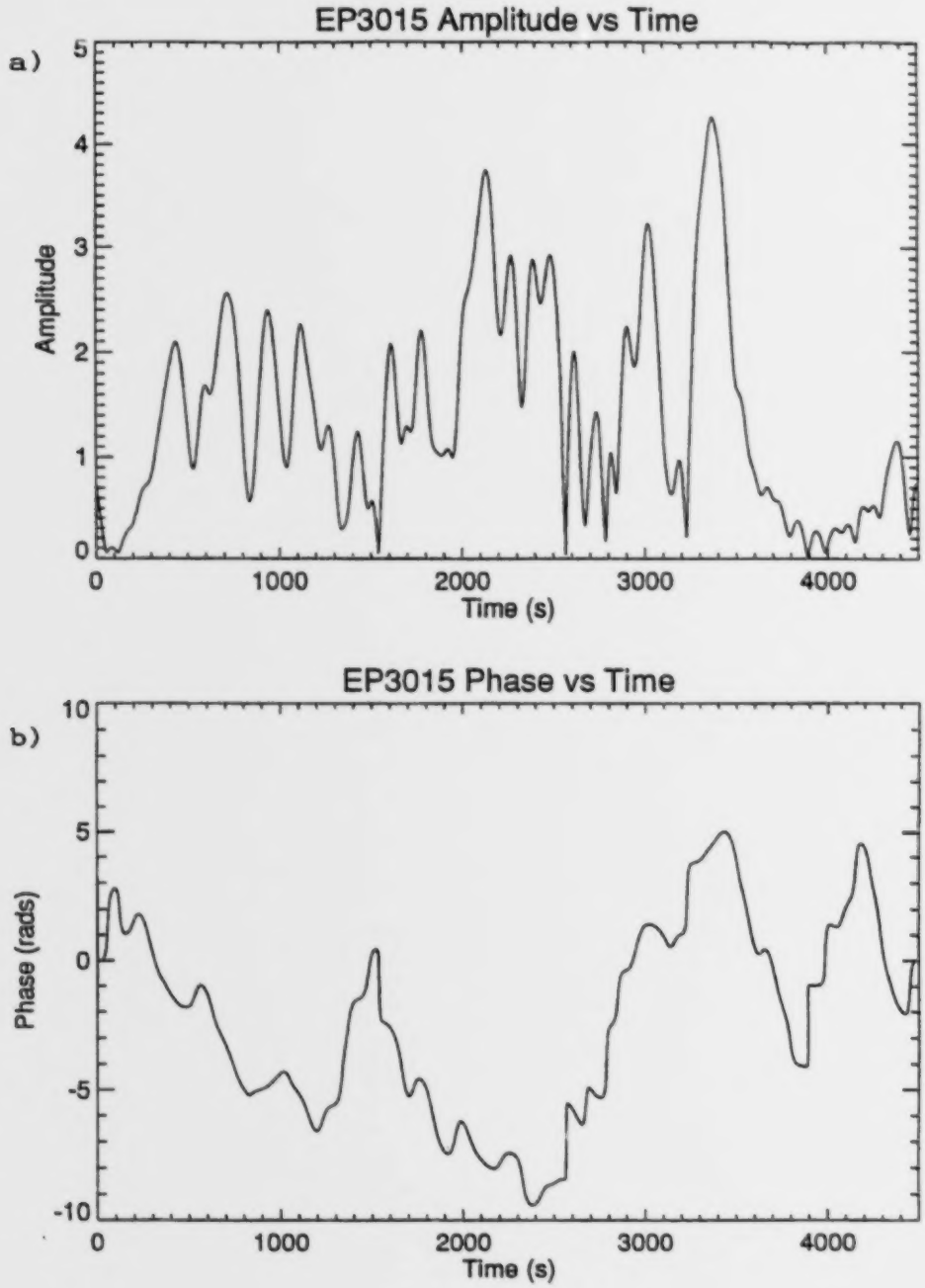

Figure A10. (a) The amplitude-vs-time of the 57 Hz signal transmitted Jan. 30 at 1500 UTC and (b) the phase-vs-time plot showing the temporal variability of this signal.

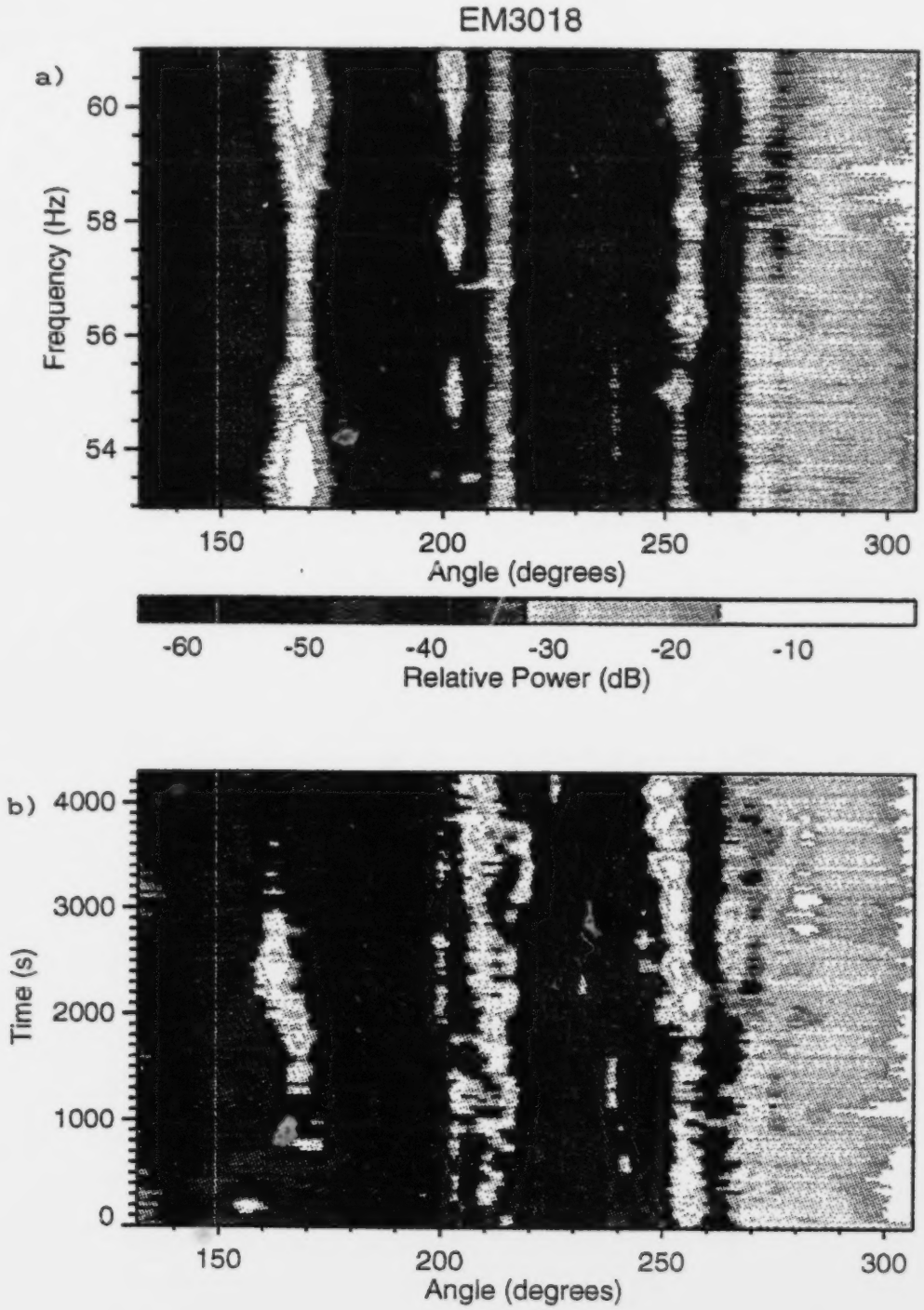

Figure A11. (a) The frequency-vs-arrival angle of the M-sequence signal transmitted Jan. 30 at 1800 UTC and (b) the beam power-vs-time plot showing the temporal variability of this signal.

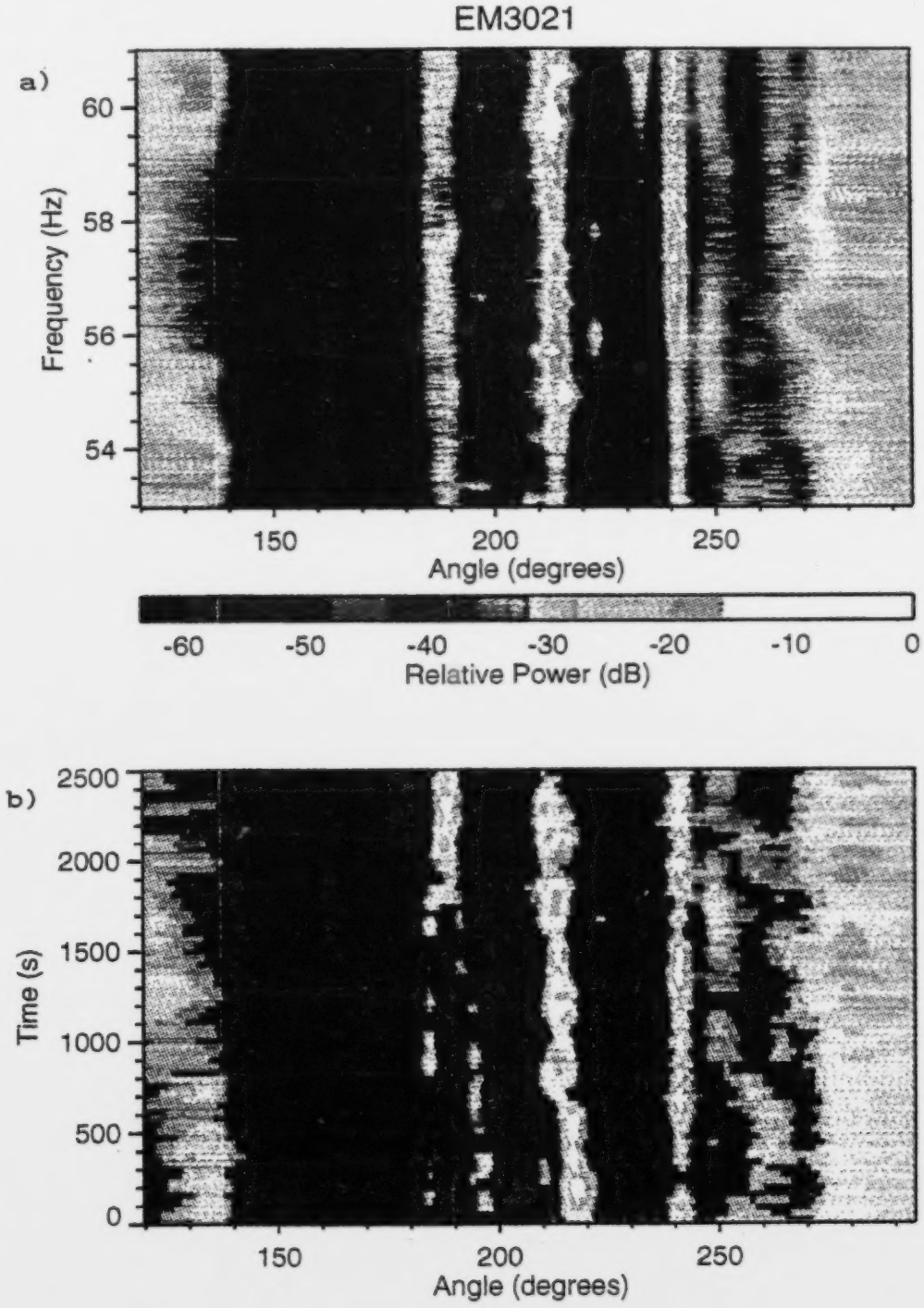

Figure A12. (a) The frequency-vs-arrival angle of the M-sequence signal transmitted Jan. 30 at 2100 UTC and (b) the beam power-vs-time plot showing the temporal variability of this signal.

Appendix B

Additional Frequency-vs-Arrival Angle

Plots

from CFAV *Quest*

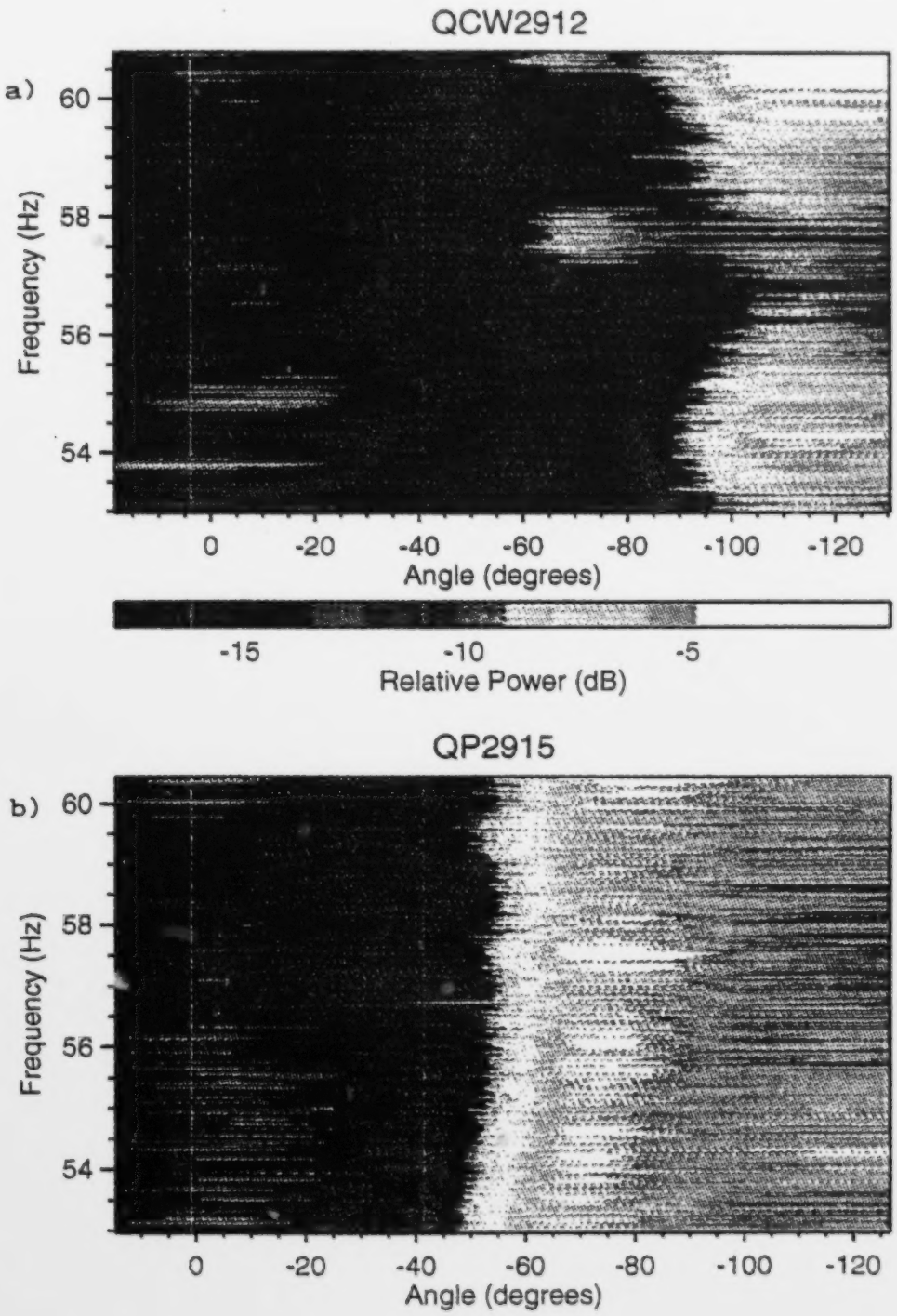

Figure B1. The frequency-vs-arrival angle plots of (a) the CW signal transmitted Jan. 29 at 1200 UTC and (b) the pentaline signal transmitted Jan. 29 at 1500 UTC. Neither plot shows a strong indication of the 57 Hz Heard Island signal.

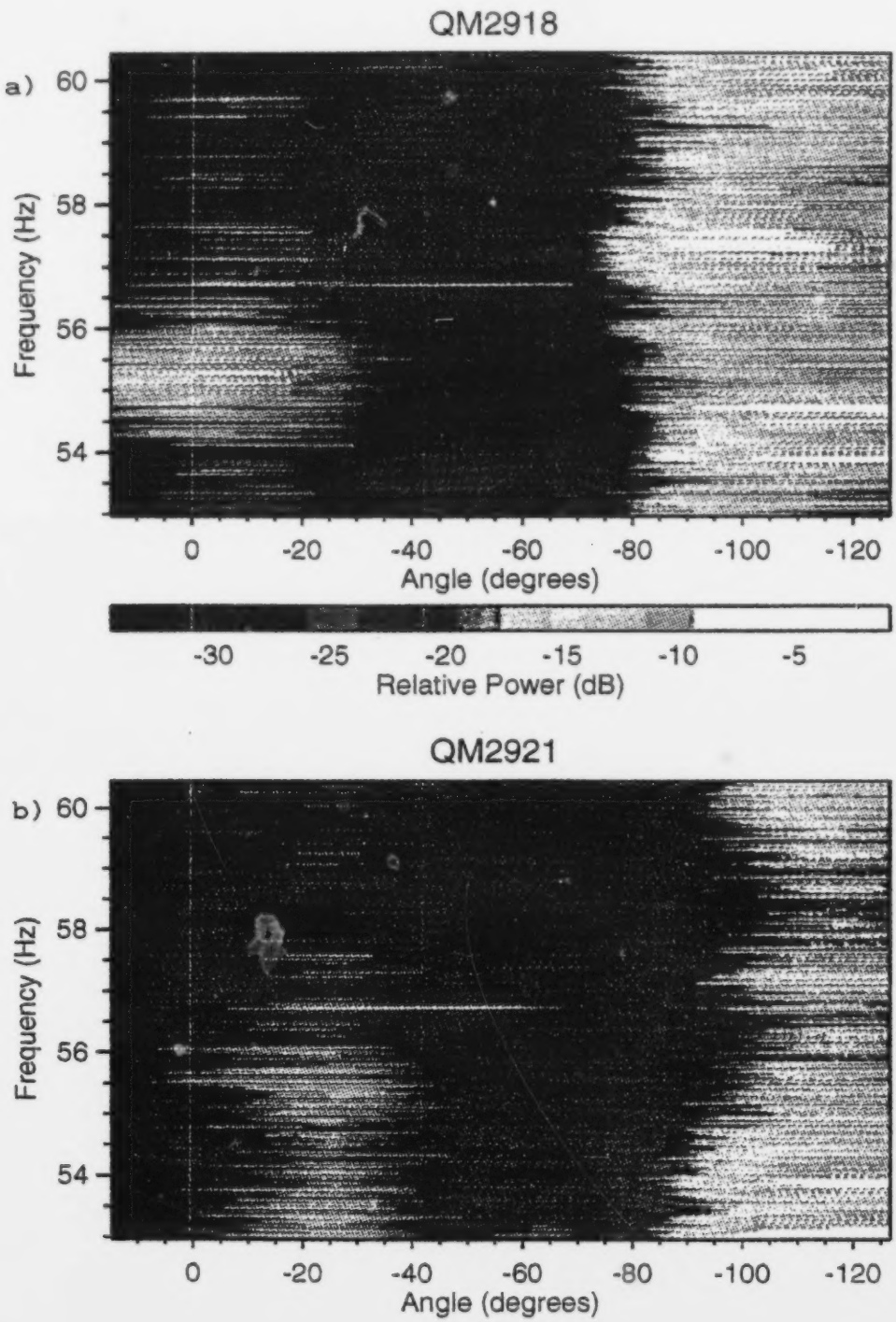

Figure B2. The frequency-vs-arrival angle plots of (a) the M-sequence transmitted Jan. 29 at 1800 UTC and (b) the M-sequence transmitted Jan. 29 at 2100 UTC. These plots both show the presence of the 57 Hz Heard Island signal.

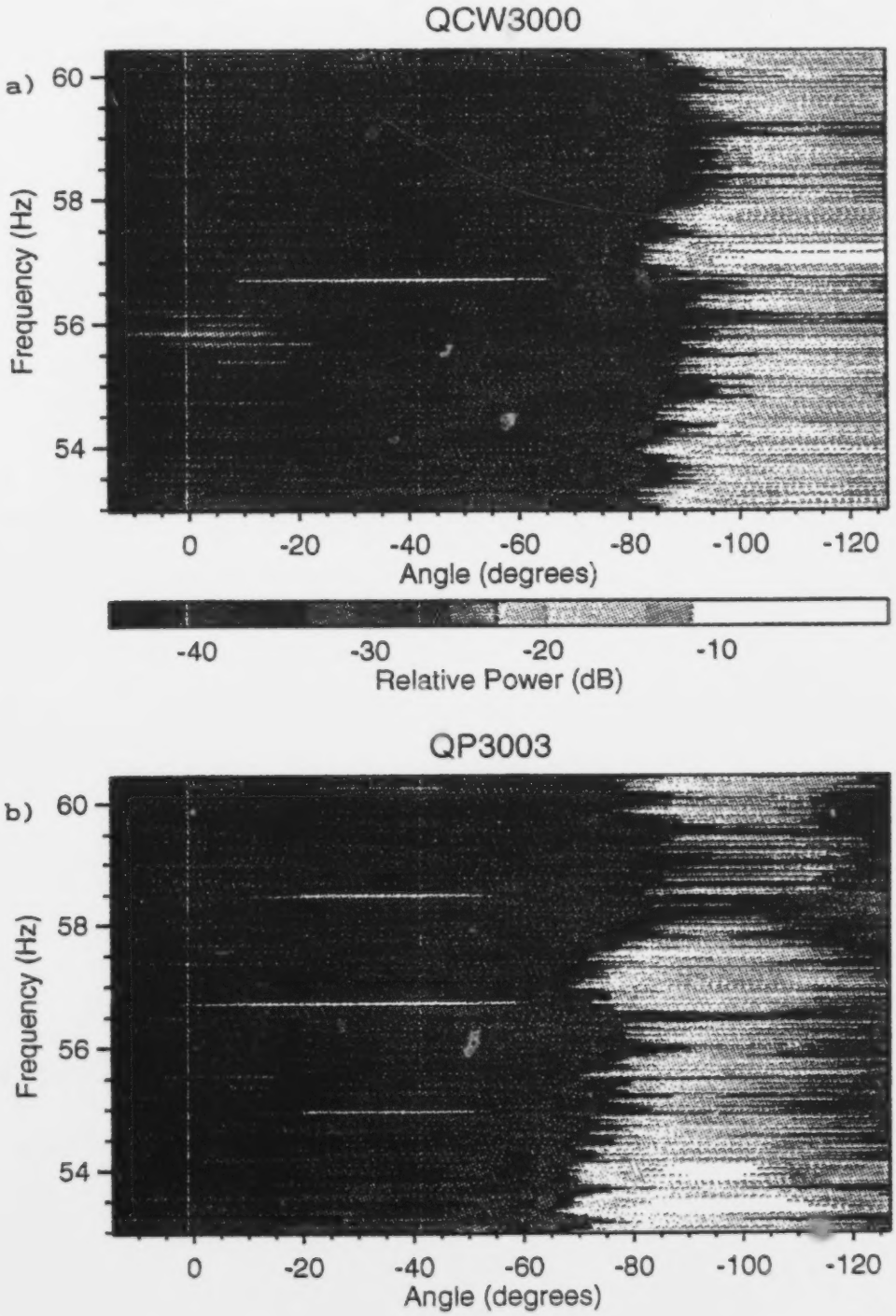

Figure B3. The frequency-vs-arrival angle plots of (a) the CW signal transmitted Jan. 30 at 0000 UTC and (b) the pentaline signal transmitted Jan. 30 at 0300 UTC. These plots both clearly show the presence of the 57 Hz Heard Island signal.

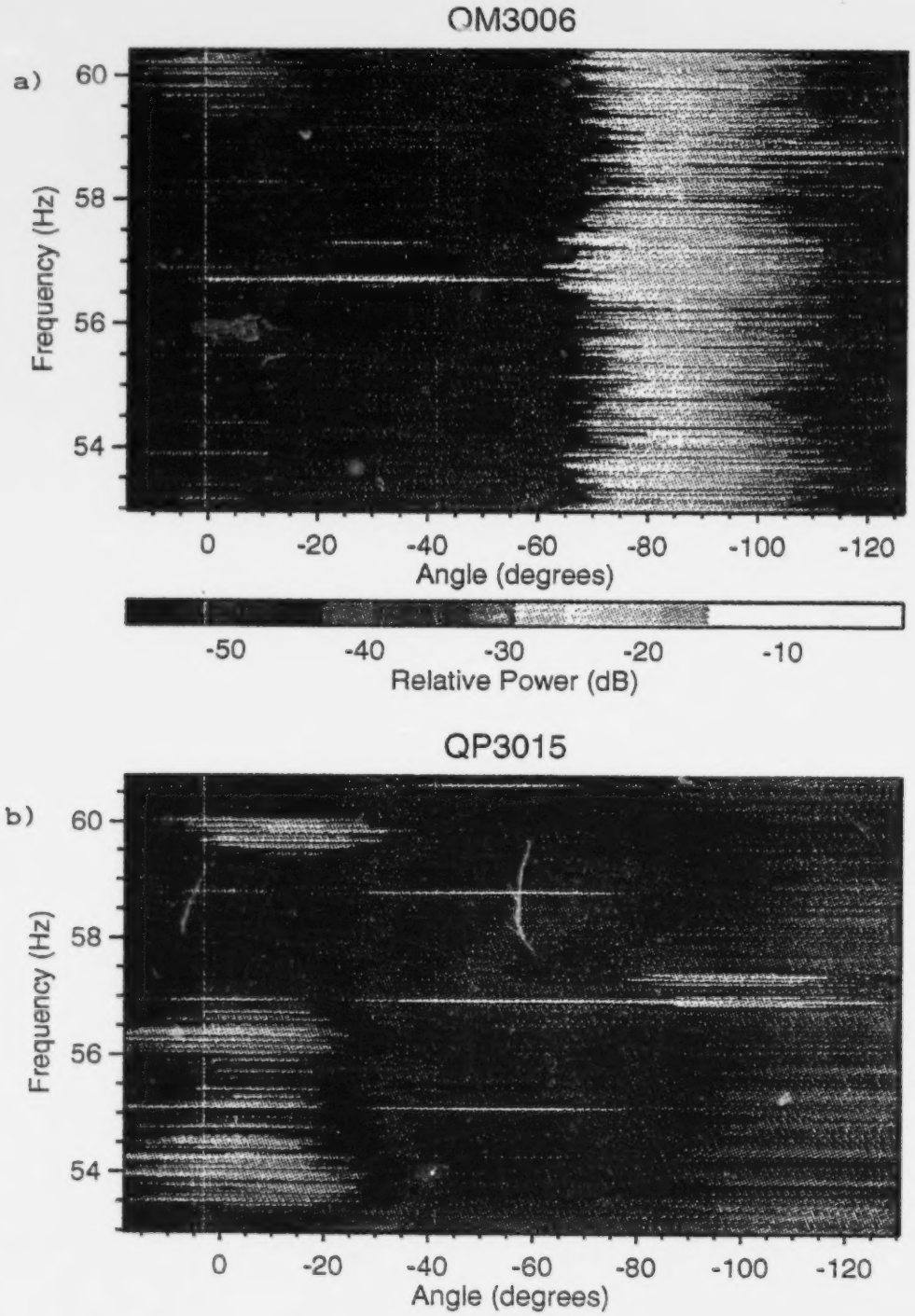

Figure B4. The frequency-vs-arrival angle plots of (a) the M-sequence transmitted Jan. 30 at 0600 UTC and (b) the pentaline signal transmitted Jan. 30 at 1500 UTC. These plots both clearly show the presence of the 57 Hz Heard Island signal.

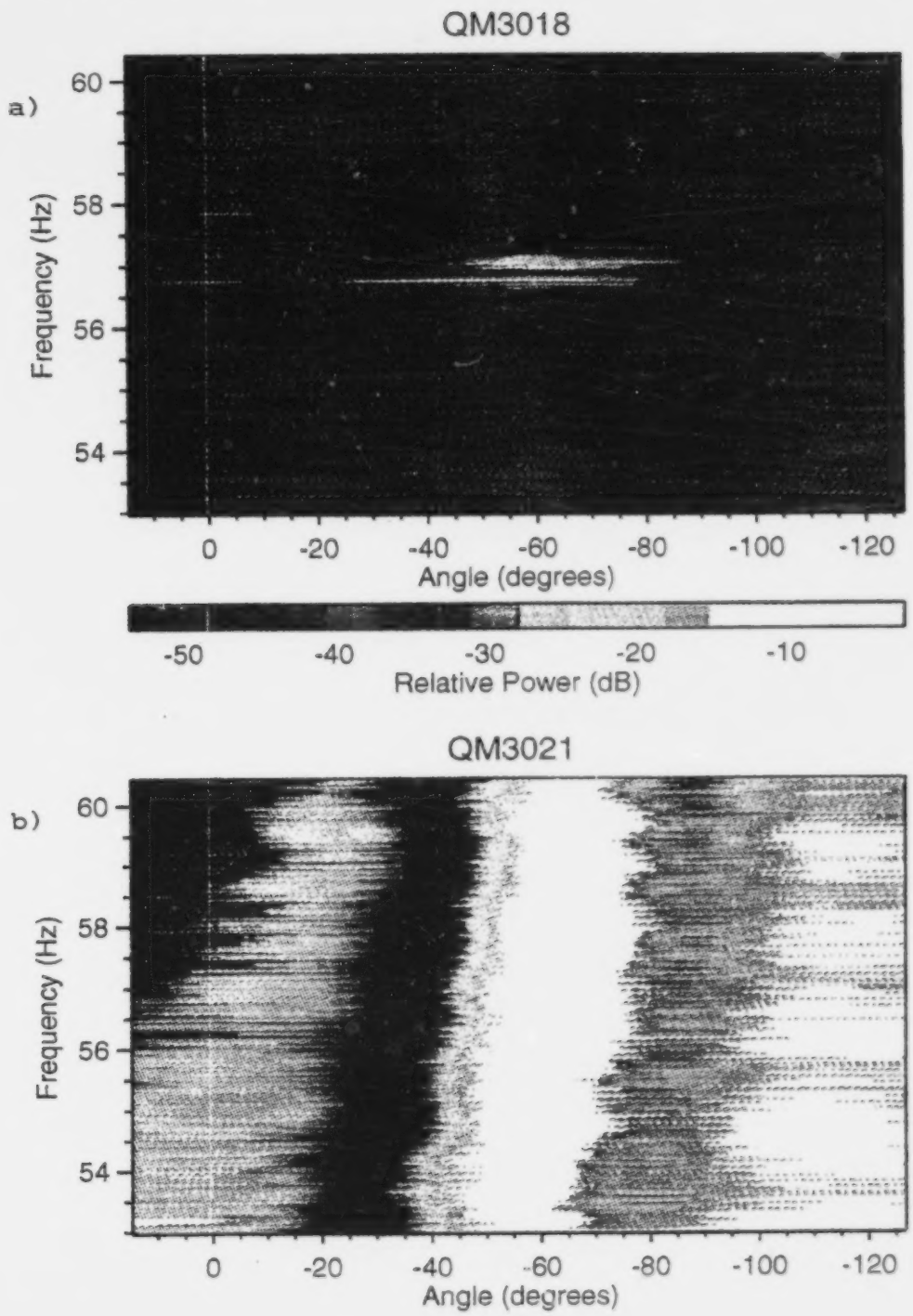

Figure B5. The frequency-vs-arrival angle plots of (a) the M-sequence transmitted Jan. 30 at 1800 UTC and (b) the M-sequence transmitted Jan. 30 at 2100 UTC. The upper plot shows a strong 57 Hz Heard Island signal, however the lower plot is swamped by interfering noise sources.

REPORT NO.: DREP CONTRACTORS REPORT SERIES 94-64

TITLE: A Summary of Acoustic Data from the Heard Island Feasibility Test Pertaining to the Canadian Receiving Stations

AUTHOR: Paul Scrimger, Ian Schumacher.
JASCO Research Ltd., Sidney, BC Canada V8L 3S1

DATED: June, 1994

SECURITY GRADING: UNCLASSIFIED

DISTRIBUTION LIST:

DSIS (2)

~~DREP Library (2)~~

Dr. Ross Chapman, DREP

DREA Library (2)

Dr. Ian Fraser, DREA

Dr. Garry Heard, DREP

Mr. Terry Curran, Fisheries & Oceans - 363-6323

Environmental Innovations Programme - 819-956-1680

Dr. McTaggart-Cowan - Province of BC , Department of Environment, Lands and Parks, 777 Broughton Street, 4th Floor, Victoria, BC V8V 1X5

Mr. Galen Greer, Province of BC, Ministry of Employment and Investment, Science & Technology Division, 2nd Floor, 1022 Government Street, Victoria, BC V8V 1X4

Mr. Ron Woodward, - Science Council of British Columbia, Suite 800, 4710 Kingsway, Burnaby, BC. V5H 4M2

Continued.....

Prof. Victor Akulichev
Institute of Marine Technology Problems
Far Eastern Branch-Russian Academy of Sciences
5a Sukhanov Str.
Vladivostok, 690600 Russia

Work (423)222-6416
FAX (423)222-6451
E-mail akulich@imtp.marine.su

Dr. Arthur Baggeroer
Department of Ocean Engineering
Massachusetts Institute of Technology
77 Massachusetts Avenue, Room 5-504
Cambridge, MA 02139 USA

Work (617)253-4366
FAX (617)253-8125
E-mail abb@arctic.mit.edu or
abb@munk.ucsd.edu

Dr. Theodore Birdsall
Communications and Signal Processing Laboratory
University of Michigan
1301 Beal Avenue
4242 EECS Building, North Campus
Ann Arbor, MI 48109-2122 USA

Work (313)936-0267
FAX (313)763-1503
E-mail ted_birdsall@ub.cc.umich.edu or
birdsall@munk.ucsd.edu

Dr. Ann Bowles
Hubbs Sea World,
1700 South Shores Road,
San Diego, CA 92109 USA

Work (619)226-3873
FAX (619)226-3944
E-mail bowles@munk.ucsd.edu or
OMNET: a.bowles

Dr. Ching-Sang Chiu
Department of Oceanography
Naval Postgraduate School
Code OC/Ci
Monterey, CA 93943 USA

Work (408)646-3239
FAX
E-mail

Dr. Geoff Brundrit
Department of Oceanography
University of Capetown
Rondebosch, 7700 South Africa

Work 27(21)650-3277
FAX 27(21)650-3979
E-mail brundrit@munk.ucsd.edu or
OMNET:capetown.ocean

Dr. Leif Bjorno
Industrial Acoustics Department
Technical University of Denmark
Building 425
Lyngby, DK 2800 Denmark

Work 45 42 882522 Ext. 4766-68
FAX 45 45 93 01 90; Home Fax 45 42522671
E-mail bjorno@munk.ucsd.edu or
OMNET:L.Bjorno

Dr. Ralph Alewine
Director, Nuclear Monitoring Research Office
Defence Advanced Research Projects Agency
3701 N. Fairfax Drive
Arlington,
VA 22203-1714 USA

Work (703)696-2203
FAX (703)696-2203
E-mail alewine@a.darpa.mil or
alewine@munk.ucsd.edu

Dr. Yves Desaubies
IFREMER/Centre de Brest
B.P. 70
Plouzane, 29280 France

Work 33 98 22 42 75
FAX 33 98 22 44 96
E-mail desaubies@munk.ucsd.edu or
OMNET:Y.Desaubies

Dr. Nikolai Dubrovsky
N. Andreyev Acoustical Institute
Shvernik Street N4
Moscow, 117036 Russia

Work (795)126-7401
FAX (795)126-8411
E-mail acin@compnet.npimsu.msk.su or
dubrovsky@munk.ucsd.edu

Dr. Andrew Forbes
CSIRO Division of Oceanography
G.P.O. Box 1538
Hobart, Tasmania Australia

Work 61-02-206300
FAX 61-02-241710
E-mail forbes@ml.csiro.au or
OMNET: A.Forbes

Mr. Warren Denner
EOS Research Associates

Work
FAX (408)659-0630
E-mail

Prof. Guan Dinghua
Institute of Acoustics Academia Sinica
17 Zhongguancun Street PO Box 2712
Beijing 100080 China

Work 86-1-256 9080
FAX 86-1-256 1457
E-mail

Dr. David Farmer
Institute of Ocean Sciences
PO Box 6000
Sidney, BC V8L 4B2 Canada

Work (604)363-6591
FAX (604)363-6798
E-mail dfarmer@sirius.uvic.ca or
farmer@munk.ucsd.edu

Dr. Garry Heard
Defence Research Establishment Pacific
Ocean Physics
FMO Esquimalt, BC V0S 1B0 Canada

Work (604)363-2905
FAX (604)363-2856
E-mail heard @orca.drep.dnd.ca

Dr. Harley Hurlburt
Naval Research Lab
Code 7320, Building 1103
Stennis Space Center, MS 39529 USA

Work (601)688-4626
FAX (601)688-4759
E-mail OMNET: H.Hurlburt

Ms. Ann Kerr
Scripps Institution of Oceanography-UCSD
IGPP-0225
La Jolla, CA 92093 USA

Work (619)534-2103
FAX (619)534-8076
E-mail kerr@munk.ucsd.edu or
OMNET:A.Kerr

Dr. David Hyde
Scripps Institution of Oceanography IGPP-0225
La Jolla, CA 92093 USA

Work (619)534-3711
FAX (619)534-8076
E-mail hyde@munk.ucsd.edu

Dr. John Kay
Defence Scientific Establishment
Auckland Naval Base
Auckland, New Zealand

Work (649)445-5870
FAX (649)445-5890
E-mail
Work
FAX
E-mail

Dr. William Kuperman
Naval Research Laboratory
Code 5160
Washington, D.C. 20375-5000 USA

Work (202) 767-9037
FAX (202) 404-7732
E-mail kuperman@munk.ucsd.edu or
OMNET: W.Kuperman

Dr. Bruce Howe
Applied Physics Lab.,
University of Washington
1013 NE 40th Street,
Seattle, WA 98105-6698 USA

Work (206) 543-9141
FAX
E-mail howe@apl.washington.edu or
OMNET:B.Howe

Dr. Khosrow Lashkhari
Monterey Bay Aquarium Research Institute
(MBARI)
160 Central Avenue
Pacific Grove, CA 93950

Work (408) 647-3731
FAX (404) 649-8587
E-mail khosrow@munk.ucsd.edu or
lakh@hp850.mbari.org

Dr. Edward McDonald
Naval Research Laboratory
4555 Overlook Avenue, SW Code 5105
Washington , D.C. 20375-5000 USA

Work (202) 767-9037
FAX (202) 404-7732
E-mail mcdonald@ccf.nrl.navy.mil or
OMNET: B.McDonald

Dr. Kurt Metzger
University of Michigan
CSPL, EECS Building, North Campus
Ann Arbor, MI 48109-2122 USA

Work (313) 764-5226
FAX
E-mail metzger@eecs.umich.edu or
OMNET: K.Metzger

Dr. Jim Miller
Assistant Professor,
Naval Postgraduate School
Department of Oceanography
Monterey, CA 93942

Work (408) 646-2384
FAX (408) 646-2760
E-mail miller@ece.nps.navy.mil or
OMNET: J.Miller.NPS

Dr. James Mercer
Applied Physics Laboratory
University of Washington
1013 NE 40th Street,
Seattle, WA 98105 USA

Work (206) 543-1361
FAX (206) 543-3521
E-mail mercer@apl.washington.edu or
OMNET:J.Mercer

Dr. Walter Munk
Scripps Institution of Oceanography-UCSD
IGPP-0225
La Jolla, CA 92093-0225 USA

Work (619)534-2877
FAX (619)534-6354
E-mail munk@munk.ucds.edu or
OMNET:W.Munk

Dr. Iwao Nakano
Ocean Research Department
Japan Marine Science & Technology Center
(JAMSTEC)
2-15 Natsushima-cho
Yokusuka, 237 Japan

Work 81-468-66-3811
FAX 81-468 66 0970
E-mail nakano@munk.ucsd.edu or
OMNET:JAMSTEC

Dr. David Palmer
NOAA Atlantic Oceanographic &
Meteorologic Laboratory,
4301 Rickenbacker Causeway
Miami, FL 33149 USA

Work (305)361-4416
FAX (305)361-4449
E-mail palmer@munk.ucsd.edu or
OMNET:AOML.MIAMI

Dr. John Penrose
Centre for Marine Science and Technology
Curtin University
Kent Street, Bentley
Perth, 6102 W. Australia

Work 61-9-351-7380
FAX 61-9-351-2377
E-mail tpenrosej@cc.curtin.edu.au

Dr. Robert Spindel
Applied Physics Laboratory
University of Washington
1013 NE 40th Street, Room 606,
Seattle, WA 98105 USA

Work (206)543-1310
FAX (206)543-3521
E-mail spindel@apl.washington.edu or
OMNET:R.Spindel

Prof. Chris T. Tindle
Physics Department
University of Auckland
Private Bag
Auckland, New Zealand

Work 64 9 373-7999x8871
FAX 64 9 373-7934
E-mail ctt@phyvc.aukuni.ac.nz or
OMNET:aunz.physics

Dr. John Spiesberger
Associate Scientist
Woods Hole Oceanographic Institution
Woods Hole, MA 02543

Work (508)548-1400x2288
FAX (508)457-2194
E-mail spiesberger@munk.ucsd.edu or
OMNET:J.Spiesberger

Dr. Peter Worcester
Scripps Institution of Oceanography,UCSD
IGPP-0213
La Jolla, CA 92093 USA

Work (619)534-4688
FAX
E-mail pworcester@ucsd.edu or
OMNET:P.Worcester

Dr. Ann Bowles
Hubbs Sea World
1700 South Shores Road
San Diego, CA 92109

Work (619)226-3873
FAX (619)226-3944
E-mail bowles@munk.ucsd.edu or
OMNET: a.bowles

Dr. Steven F. Clifford
Director, Wave Propagation Laboratory
National Oceanic & Atmospheric Administration,
ERL
325 Broadway R/E/WP
Boulder, CO 80303-3328

Work (303) 497-6291
FAX (303) 497-6020
E-mail

Dr. Irina N. Kozhevnikova
Department of Industrial Acoustics
Technical University of Denmark
Building 425
Lyngby, DK-2800 Denmark

Work 45 42 88 25 22
FAX 45 45 93 01 90
E-mail

Dr. Bernard Massinon
Laboratoire de Detection et de Geophysique
Commissariat a l'Energie Atomique
Bruyere-le-Chatel, BP 12 91680 France

Work 33 1 69 26 50 59
FAX 33 1 69 26 60 49
E-mail

Dr. C.S. Murty
National Institute of Oceanography
Dona Paula, Goa 403 004 India

Work
FAX 91-0 832-44612
E-mail

Dr. Marshall Orr
Office of Naval Research
800 N. Quincy Street - Code 1125 OA
Arlington, VA 22217-5000 USA

Work (703) 696-6994
FAX (703) 696-4884
E-mail orr@munk.ucsd.edu or
OMNET: M.Orr

UNCLASSIFIED

SECURITY CLASSIFICATION OF FORM
(highest classification of Title, Abstract, Keywords)

DOCUMENT CONTROL DATA

(Security classification of title, body of abstract and indexing annotation must be entered when the overall document is classified)

1. ORIGINATOR (the name and address of the organization preparing the document. Organizations for whom the document was prepared, e.g. Establishment sponsoring a contractor's report, or tasking agency, are entered in section 8.)

Jasco Research Ltd.
#205 - 9865 West Saanich Road,
Sidney, BC. Canada. V8L 3S1

2. SECURITY CLASSIFICATION (overall security classification of the document including special warning terms if applicable)

UNCLASSIFIED

3. TITLE (the complete document title as indicated on the title page. Its classification should be indicated by the appropriate abbreviation (S,C or U) in parentheses after the title.)

Analysis of Acoustic data from the Heard Island Feasibility Test Pertaining to the Canadian Receiving Stations.

4 AUTHORS (Last name, first name, middle initial)

Scrimger, Paul
Schumacher, Ian

5. DATE OF PUBLICATION (month and year of publication of document)

June, 1994

6a. NO. OF PAGES (total containing information. Include Annexes, Appendices, etc.)

39

6b. NO. OF REFS (total cited in document)

11

7. DESCRIPTIVE NOTES (the category of the document, e.g. technical report, technical note or memorandum. If appropriate, enter the type of report, e.g. interim, progress, summary, annual or final. Give the inclusive dates when a specific reporting period is covered.)

DREP Contractor's Report 94-64

8. SPONSORING ACTIVITY (the name of the department project office or laboratory sponsoring the research and development. Include the address.)

DREP
DREA

9a. PROJECT OR GRANT NO. (if appropriate, the applicable research and development project or grant number under which the document was written. Please specify whether project or grant)

9b. CONTRACT NO. (if appropriate, the applicable number under which the document was written)

W7708-2-0518/01-XSA

10a. ORIGINATOR'S DOCUMENT NUMBER (the official document number by which the document is identified by the originating activity. This number must be unique to this document.)

94-64

10b. OTHER DOCUMENT NOS. (Any other numbers which may be assigned this document either by the originator or by the sponsor)

11. DOCUMENT AVAILABILITY (any limitations on further dissemination of the document, other than those imposed by security classification)

(X) Unlimited distribution
( ) Distribution limited to defence departments and defence contractors; further distribution only as approved
( ) Distribution limited to defence departments and Canadian defence contractors; further distribution only as approved
( ) Distribution limited to government departments and agencies; further distribution only as approved
( ) Distribution limited to defence departments; further distribution only as approved
( ) Other (please specify):

12. DOCUMENT ANNOUNCEMENT (any limitation to the bibliographic announcement of this document. This will normally correspond to the Document Availability (11). However, where further distribution (beyond the audience specified in 11) is possible, a wider announcement audience may be selected.)

UNCLASSIFIED

UNCLASSIFIED

SECURITY CLASSIFICATION OF FORM

5. ABSTRACT (a brief and factual summary of the document. It may also appear elsewhere in the body of the document itself. It is highly desirable that the abstract of classified documents be unclassified. Each paragraph of the abstract shall begin with an indication of the security classification of the information in the paragraph (unless the document itself is unclassified) represented as (S), (C), or (U). It is not necessary to include here abstracts in both official languages unless the text is bilingual).

This report provides a summary of the acoustic data associated with the Canadian measurements taken during the Heard Island Feasibility Test. It is the sixth and final report in a series of reports and journal articles which have been produced under DSS contract no. W7708-2-0518/01-XSA. The other reports produced under this contract included a summary of non-acoustic data from the Heard Island Feasibility Test pertaining to the Canadian receiving stations, three consecutive articles submitted to the Journal of the Acoustical Society of America (JASA) describing novel signal processing techniques developed during the course of this work and a DREP contractors report which investigated the optimum location for a receiving array off Canada's west coast for ATOC (Acoustic Thermometry of Ocean Climate).

6. KEYWORDS, DESCRIPTORS or IDENTIFIERS (technically meaningful terms or short phrases that characterize a document and could be helpful in cataloguing the document. They should be selected so that no security classification is required. Identifiers, such as equipment model designation, trade name, military project code name, geographic location may also be included. If possible keywords should be selected from a published thesaurus, e.g. Thesaurus of Engineering and Scientific Terms (TEST) and that thesaurus identified. If it is not possible to select indexing terms which are Unclassified, the classification of each should be indicated as with the title.)

HIFT
GLOBAL WARMING

UNCLASSIFIED.